BELBaR

(Contract Number: FP7 *295487*)

Understanding of Radionuclide Colloid Interaction
(with special emphasis on sorption reversibility)
DELIVERABLE D3.3

Authors:

Nick Bryan and Nick Sherriff, University of Manchester

Reporting period: **01/03/12 – 29/02/16**
Date of issue of this report: **27/05/13**
Start date of project: **01/03/12**
Duration: **48** Months

DISTRIBUTION LIST

Name	Number of copies	Comments
Christophe Davies (EC) BELBaR participants		

1   Introduction

This report describes the progress in the BELBaR project in the field of radionuclide bentonite colloid interactions. It starts with a summary of a review of the understanding of the reversibility of the interactions of radionuclides with bentonite (bulk and colloidal) before the start of the project. There follows a description of work published by the BELBaR partners since the start of the project and also the results of the current BELBaR experimental programmes.

Important Caveat: For the data that have not yet been published in the open literature, the results reported here are **<u>preliminary</u>** and are subject to later reanalysis and reinterpretation. In particular, many of the BELBaR experiments are long-term studies to determine rate constants. In order that the current state of progress is clear, we have reported rate constants that have been calculated from the current data sets. However, these experiments are continuing, and as further data points are produced, **the values of the rate constants may change**. It is not intended that the unpublished rate constants reported here should be used, for example in support of a safety case.

Following the description of the current state of work, there is a discussion of the current understanding of the reversibility of radionuclide-bentonite colloid interactions and the implications for radionuclide mobility in the vicinity of a high level radioactive waste repository with a bentonite backfill.

This work contains information on radionuclide-bentonite interactions only. There are of course other important processes that will affect the probability of bentonite colloid assisted transport, for example colloid stability, but these are discussed elsewhere.

2 Review of Existing Literature

Before the start of experimental work in the BELBaR project, a thorough literature review was undertaken to determine the state-of-the-art. This section contains a summary of that review.

2.1 The role of colloids in radionuclide transport

The importance of colloids in aiding the transportation of radionuclides depends on a number of factors. The type of bentonite and even the future climate, such as glacial melts altering the groundwater chemistry, could affect the importance of colloid mediated transport (Wold 2010). The various factors have been combined in the so called 'Colloid Ladder' (Mori et al 2003), which is shown schematically in Figure 1.
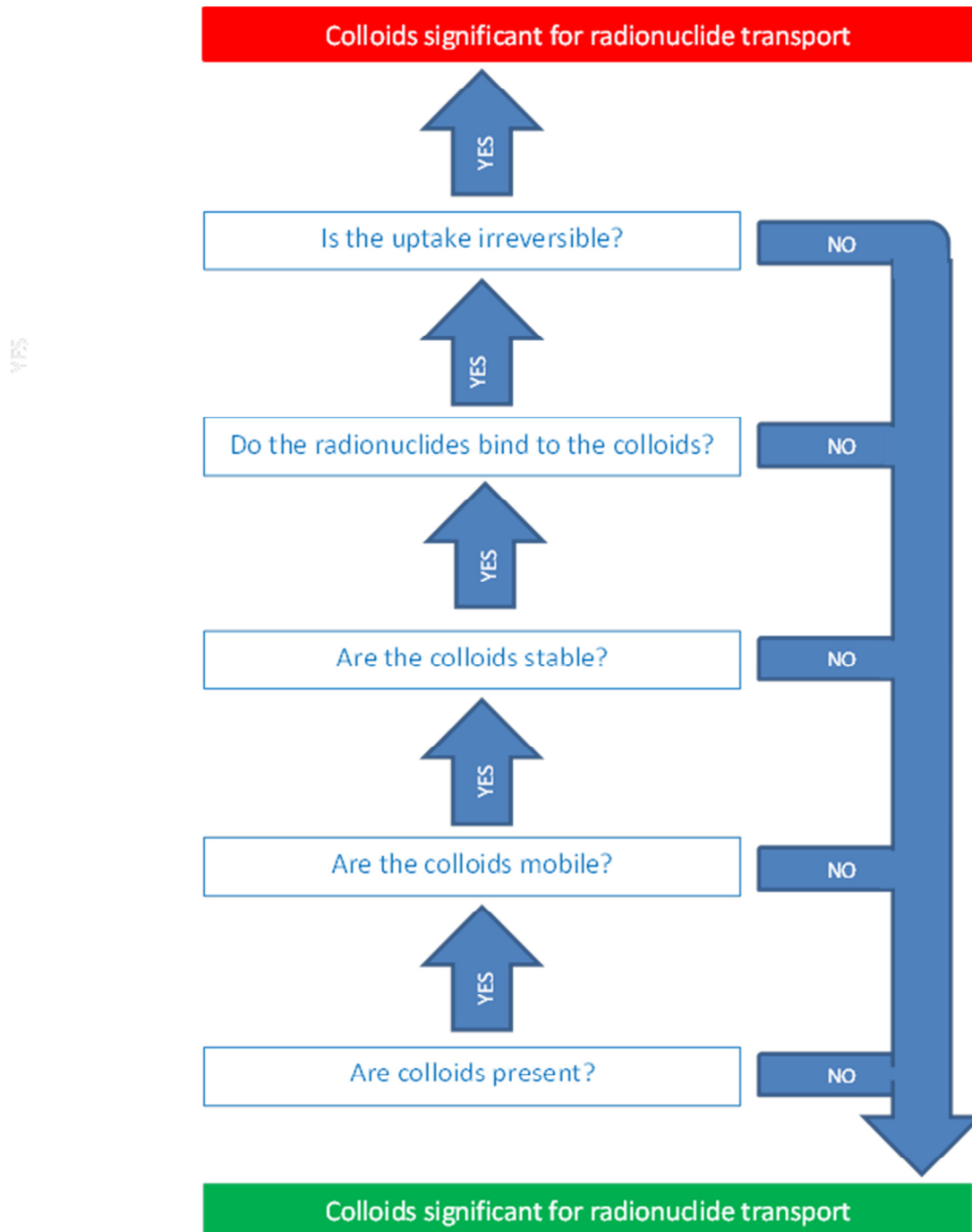

Figure 1. The colloid ladder (Mori et al 2003).

For colloidal transport to be significant, all of the following factors must be considered (Mori et al 2003; Missana et al 2008; Honeyman 1999; Miller et al 1994; Ryan and Elimelech 1996):

- **Are colloids present?** - If colloids are not present in the system, then they will not be able to promote radionuclide mobility, but if they are, then they may.
- **Are the colloids mobile?** – If the colloids themselves are not mobile, then they will not be able to promote radionuclide mobility.
- **Are the colloids stable?** - If the colloids are unstable, then any associated radionuclides would be removed from the mobile phase (the solution) as the colloids are destabilised.
- **Is there radionuclide uptake?** – If radionuclides do not bind to the colloids at all, then the colloids cannot promote transport.
- **Is uptake irreversible?** – If the binding of the radionuclide to the colloid is reversible, then colloids should not be significant for radionuclide transport, because the rock itself should be able to compete for binding of the radionuclide. If the binding were to be irreversible however, then transport of the radionuclide would essentially continue until the colloid stopped moving.

For colloids to be significant in the transport of radionuclides, then the answers to each of the questions listed above must be 'yes'. Here we will concentrate only on the last of these points (irreversibility).
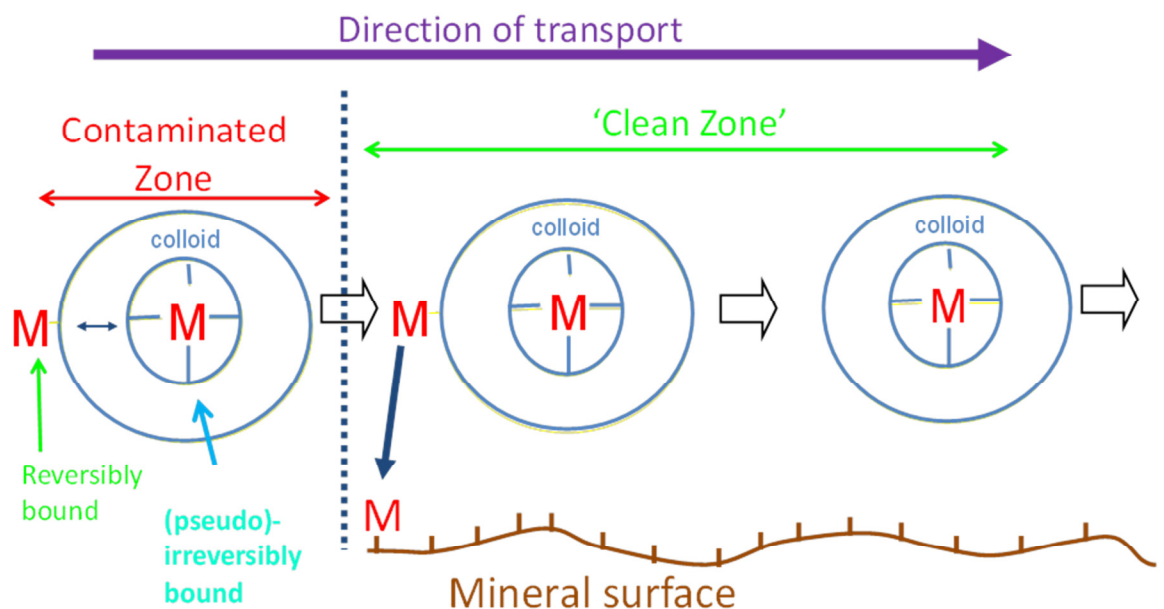

Figure 2: The mechanism for the transport of 'irreversibly' bound radionuclides (M).

Figure 2 shows the mechanism for the transport of irreversibly bound radionuclides. If colloids encounter radionuclides in a contaminated region, for example in or near a repository, then it is possible that they could become bound to the colloid, either reversibly or irreversibly. If the colloid then moves away, for example a bentonite colloid transporting through a fracture, then it would carry those bound radionuclides with it. However, it is expected that any radionuclides that are bound reversibly, and so may dissociate instantaneously, would be quickly and easily removed by the available rock surface binding sites that will be present in excess. In the case of irreversibly bound radionuclides, the strength of the competing sink will not remove the radionuclides, and the radionuclide will be transported with the colloids.

2.2   Radionuclide interactions with bulk bentonite

The interactions of radionuclides with bulk bentonite (and its constituents) have been studied extensively (Wold 2010). For example, Stumpf et al (2004) used TRLFS and EXAFS to study the coordination of trivalent actinide ions by the bulk. At ambient pH, they found that inner sphere complexes were formed with bonds to 4 oxygens on the surface, and approximately five waters retained. Rabung et al (2005) found a similar result for Eu(III) and Cm(III), with three different surface complexes, each with five waters/hydroxides in the coordination environment (as well as the surface oxygens): the number of hydroxides increases with pH. At very high pH (>12), Cm(III) forms a surface precipitate.

A number of models have been developed to explain and predict radionuclide surface complexation on bentonite (montmorillonite), e.g. Kowal et al (2004), but the two site protolysis non-electrostatic surface complexation and cation exchange (2SPNE SC/CE) model of Bradbury and Baeyens has proved particularly successful (e.g. Bradbury and Baeyens 1999; Bradbury et al 2005; Bradbury and Baeyens 2009; and refs therein). In this model, there are three inner sphere surface complexes for the trivalent actinides/lanthanides, $\equiv$SO-An^{2+}, $\equiv$SO-An(OH)$^+$ and $\equiv$SO-An(OH)$_2$, in addition to ion exchange sites. Unlike many surface complexation models, it is quasi-mechanistic: there is spectroscopic evidence for the predicted surface speciation (e.g., Rabung et al 2005) and there is a convincing correlation between the model equilibrium constants and radionuclide hydrolysis constants (Bradbury and Baeyens 2006).

Guo et al (2009) studied sorption and desorption of Eu(III) to bulk (Na)-bentonite, and found that for the bulk, the interaction was reversible over a period of a week. Only the irreversibility of Cs binding to bulk clays has been studied extensively (e.g., Comans, 1987; Comans et al., 1991; de Koning and Comans, 2004).

2.3   Radionuclides and colloidal bentonite and reversibility

Theoretical calculations by NAGRA (NAGRA, 1994) have shown that 'irreversibility' associated with colloidal ternary systems may significantly influence radionuclide mobility from a repository. Further, inorganic colloids have been implicated in the enhanced migration of radionuclides in the environment (Kersting et al 1999). It has been found that under the correct conditions, bentonite colloid associated radionuclides can travel faster than a conservative tracer (Geckeis et al 2004). Calculations have shown that the slow dissociation of radionuclides from solution phase colloids (short of 'irreversibility') can result in the rapid transport of radionuclides: in order to have an effect, the residence time of the colloidal material in the solution only needs to be less than the half time of the dissociation reaction, migration increasing with reaction half-time (Bryan et al 2007). The effect of slow dissociation kinetics (and colloid sorption) may be assessed using an approach based on Damkohler numbers (Bryan et al 2007).

Although radionuclide uptake onto bulk bentonite and montmorillonite have been studied extensively, sorption to bentonite colloids has not, and the critical dissociation kinetics barely at all (Wold 2010). Geckeis et al (2004) determined K_d values for uptake onto bentonite colloids of $1.2 \times 10^6 - 2.7 \times 10^6$ l kg^{-1} for Am(III) and $1.0 \times 10^5 - 8.0 \times 10^5$ l kg^{-1} for Pu(IV). The values for Cs(I) and U(VI) are significantly lower, $6.4 \times 10^3 - 8.7 \times 10^3$ l kg^{-1} and $0.8 \times 10^3 - 2.5 \times 10^3$ l kg^{-1}, respectively. The data for Am(III) are in the range for bulk montmorillonite, suggesting that the sorption mechanisms are similar, but Mori et al (2003) suggest that the values for Am(III) and Pu(IV) are slightly higher than for bulk bentonite, which they attribute to the larger specific surface area. Further, although the sorption strength seems constant with time for Am(III), Mori et al (2003) report an increase of an order of magnitude over the course of 3 weeks for Pu(IV). Interestingly, the TRLFS spectrum of Cm(III) bound to (FEBEX) bentonite colloids, suggests a surface complex of the form $\equiv$SO$-$Cm(H$_2$O)$_{5-x}$(OH)$_x$ (x $\leq$5), which is similar to that of Cm sorbed to bulk montmorillonite (see above; Geckeis et al 2004). There was also evidence for complexation by

organic material naturally present in the bentonite (Geckeis et al 2004). For Am(III) and Pu(IV), the strong interaction with bentonite colloidal material is sufficient to reduce the apparent K_d for sorption to the bulk rock by an order of magnitude. Missana et al (2008) have also measured K_d values for Eu(III), 5.6×10^5 - 8.1×10^5 l kg^{-1}, and Pu(IV), 1.5×10^5 - 3.5×10^5 l kg^{-1}. Wold (2010) collated experimental colloid K_d values: for Am(III) values lie in the range 10^4 - 2×10^8 l/kg , whilst those for Pu(IV) range between 1 - 2.3×10^5 l kg^{-1}, and for U(VI) the range is 8.1×10^2 - 1.6×10^3 l kg^{-1}.

Although models based on instantaneous equilibrium have been proposed for the prediction of radionuclide movement through bulk bentonite (e.g. Ochs et al 2003), kinetic processes are thought to be significant for bentonite colloid mediated transport. Experiments with actinides and technetium with bentonite colloids in the presence of fracture filling material showed 2 distinct types of behaviour: U(VI), Np(V) and Tc(VII) did not associate with the bentonite derived colloids, but Th(IV), Pu(IV) and Am(III) did (Bouby et al 2010A; Huber et al 2011). When the colloids were contacted with fracture fill material, dissociation was observed, which started after 100 - 300 hrs of contact and continued over 1000s of hours. There was some evidence that the system was approaching equilibrium after approx. 7,500 hours (Bouby et al 2010A; Huber et al 2011). Huber et al (2011) have provided dissociation rate constants for these experiments. For Am(III), the values were in the range 0.0037 - 0.009 hr^{-1} (1 - 2.5 $\times 10^{-6}$ s^{-1}), whilst for Pu(IV), the range is 0.0014 - 0.0085 hr^{-1} (3.9 $\times 10^{-7}$ - 2.4 $\times 10^{-6}$ s^{-1}). The apparent initiation period for dissociation contrasts with the behaviour for naturally occurring organic colloids, where a range of dissociation constants are observed, and dissociation commences immediately upon contact with a stronger sink (King et al 2001; Monsallier et al 2003). Wold (2010) has also estimated representative first order dissociation rate constants (k_b) for: Pu(IV) 4.35×10^{-3} hr^{-1} (= 1.2×10^{-6} s^{-1}); Am(III) 2×10^{-3} hr^{-1} (= 5.6×10^{-7} s^{-1}); Np(IV) 4.6×10^{-7} hr^{-1} (= 1.2×10^{-10} s^{-1}); Cm(III) 6×10^{-3} hr^{-1} (= 1.7×10^{-6} s^{-1}); U(VI) 3×10^{-3} hr^{-1} (= 8.3×10^{-7} s^{-1}); Tc(IV) 0.63 - 15 hr^{-1} (= 1.75×10^{-4} - 4.2×10^{-3} s^{-1}). However, these values were estimated from sorption rate constants (k_f) and assuming that $K_d = k_f/k_b$, and so they must be treated with care.

Bouby et al (2010B) found that for Eu(III), Tb(III) and Th(IV) ions, the colloid associated fraction was in the range 95 – 100 %, which was in agreement with the work of Missana et al (Missana et al 2008), which showed > 75% colloid bound for Eu(III) and Pu(IV). Schäfer et al. (2004) found that approximately 80% of Th(IV) and Eu(III) were colloid associated. Despite the apparent similarity in their amounts associated with colloids, transport experiments through a Grimsel rock core found that Th(IV) was more permanently associated with the clay colloids during transport than Am(III) and Tb(III). In fact, in a series of experiments, the Th(IV) was found to elute with the colloids. Bouby et al (2010B) suggest that there is a relationship between residence time and An(IV) (and colloid) recovery by comparison of their data with the data of: Hauser et al. (2002); Möri et al. (2003); Geckeis et al. (2004); Missana et al. (2003); Schäfer et al. (2004); Missana et al. (2008). Although there did seem to be slow dissociation, there was no evidence for irreversible binding of radionuclides, and over a period of the order of a year, equilibrium partition between colloid and fracture fill seemed to be established. Bouby et al (2010C) found that there appeared to be a discrepancy between the rates from batch and column experiments, with dissociation rates higher in transport experiments than in batch, but the reason was unclear. Transport calculations on the field scale for flow through fractures suggested that, provided the dissociation rate is greater than 0.2 yr^{-1} (6.34×10^{-9} s^{-1}), then the kinetics do not have a significant effect on radionuclide mobility, although the limit will actually depend upon the distance of interest and the flow rate (see Section 4). The authors suggested that future research should concentrate on processes that could result in such very slow dissociation (e.g. coprecipitation).

Geckeis et al (2004) found that Am(III) and Pu(IV) transport through fractures could only be explained by slow dissociation from colloids, although the interactions were eventually reversible on a time scale of months. The mechanism for slow dissociation was unclear: slow diffusion from pores could be responsible for slow Cs/Sr(II) dissociation, but it was suggested that slow break-up of surface complexes was a possible explanation for f-block ions. In lab (core) column

experiments, Missana et al. (2008) found that Eu(III) transported associated to colloids, but dissociation did take place during transport. Taking into account the residence time of the colloid associated Eu, the percentage recovery of the colloids and the amount of Eu that was associated with the colloids, it is possible to estimate an overall first order dissociation rate constant (4.8×10^{-4} s^{-1}). This is higher than rates from batch experiments (see above), but it does match with the discrepancy between column experiment and batch rates observed by Bouby et al (2010C). For Pu(IV), the recovery could be predicted directly by the colloid recovery, which could suggest that the dissociation of Pu(IV) may be slower. Given that no dissociation was observed in the column experiment, it is not possible to calculate a dissociation rate for Pu(IV), but it is possible to estimate an upper limit. Given the residence time in the column, if the minimum Pu dissociation that could be observed were 10%, then the rate constant must be less than 10^{-5} s^{-1}. The data of Missana et al (2008) show the importance of dissociation kinetics, since the same authors measured a slightly higher K_d for Eu(III) onto the colloids ($\Delta\log Kd = 0.46$). Iijima et al (2010) observed slow dissociation of bentonite colloid associated Am in a granite ternary system, but no evidence for 'irreversibility'. Interestingly, they too found that the bulk rock K_d was reduced by approximately an order of magnitude when granite was added to Am pre-equilibrated with the colloids. Delos et al (2008) studied the transport of bentonite colloids through a ceramic column. They showed that larger colloids eluted first. Am(III) and Pu(IV) elution was closely related to that of the colloids, although the Am and Pu recovery was less than that of the colloids themselves, which was interpreted as evidence of dissociation during the experiment.

Bouby et al (2011) found that Cs(I) and U(VI) did not bind to bentonite colloids, but once again the tri- and tetravalent f-block ions (Eu^{3+}; Th^{4+}) were strongly associated with the colloids. The Th(IV) was preferentially associated with the smaller colloids, which was attributed to their larger specific surface area. They also studied the competition between bentonite colloids and humic acid. In the case of Eu(III), they found that although dissociation from the inorganic colloids was slow, equilibrium was eventually obtained, and most of the Eu(III) dissociated from the bentonite colloids and bound to the humic. Most importantly, the eventual distribution was the same as that in experiments where the Eu was not pre-equilibrated with the bentonite colloids. However, in the case of Th(IV), even after 3 years, the amount of Th bound to the bentonite colloids was greater than that in a system where Th(IV) had not been pre-equilibrated with them. Therefore, for this ion at least, there does seem to be some 'irreversibility' on a time scale of 3 years. The reasons for this irreversibility are unclear, but the authors suggest that it might be due to the formation of a surface precipitate. Interestingly, Morton et al (2001) used XAS to study Cu surface coordination to bulk montmorillonite. They found that under the conditions where 'irreversibility' was observed, Cu - Cu interactions were observed. The authors interpreted the data in terms of the sorption of Cu dimers.

Wold (2010) has suggested than radionuclide ions attached to colloids via an ion exchange mechanism are unlikely to transport, because dissociation is instantaneous, and the far-field rock surface area is much larger. It is more likely that radionuclides sorbed by inner sphere surface complexation will show slow dissociation kinetics and so will be transported. That said, although slow dissociation would be possible for inner sphere surface complexes, 'irreversibity' would not be expected (Schäfer (2012).

Beyond bentonite colloids that are produced by erosion of the clay, there is the possibility of colloid formation where the bentonite pore water mixes with the background groundwater (Kunze et al 2008). Kunze et al (2008) studied the mixing of bentonite (FEBEX) pore water and Grimsel groundwater. They showed that Th(IV), Eu(III) and Cm(III) could be significantly colloid associated in the mixing zone. This result is significant, because as well as providing 'new' colloids that could act as a transport vector for radionuclides, there is the possibility that radionuclides could be incorporated as they form. Incorporation is more likely to result in very slow (pseudo irreversible) dissociation than simple surface complexation.

Therefore, slow dissociation kinetics can enhance the transport of radionuclides. Further, there is some evidence of very slow dissociation of tetravalent actinide ions under certain conditions, which could have significant consequences for actinide transport. Unfortunately, the mechanisms are not understood, and currently reliable predictions of radionuclide mobility are not possible.

3   Experimental Data From BELBaR Partners

This section describes the work from the BELBaR partners that has been published since the start of the project and also current experiments.

A running theme through all of this experimental work is the concept of competition. The study of the uptake by bentonite is relativey straightforward, and requires only that the radionuclide is introduced to the clay. However, to study the reversibility of the interaction, it has been necessary to allow the radionuclide to interact with the bentonite before using a competing ligand as a strong sink to 'pull' the radionuclide from the bentonite, so that the dissociation rate may be measured.

There is direct spectroscopic evidence that the interaction of radionuclides with bentonite colloids is the same as that with bulk material. It is easier to study radionuclide binding by bulk material than colloidal, because of the straightforward phase separation. Hence, much of the early work in BELBaR has focussed on the reversibility of radionuclide sorption to bulk bentonite, because surface complexation and incorporation effects will be the same for both.

3.1   Interactions of ^{237}U/^{237}Pu with Bentonite

The authors involved in the work in this section are: P.Ivanov,[1] T. Griffiths,[1] N.D. Bryan,[1] G. Bozhikov,[2] S. Dmitriev[2] (*1 = Centre for Radiochemistry Research, School of Chemistry, University of Manchester, Manchester, U.K.; 2 = Flerov Laboratory of Nuclear Reactions, JINR, 141980 Dubna, Russia*). The U data described in this section has been published in the open literature (Ivanov P., Griffiths T., Bryan N.D., Bozhikov G., Dmitriev S., J. Environ. Monit. 2012, 14, 2968 - 2975), but **not** the Pu work.

In these experiments, the short lived γ-emitting isotopes, ^{237}U and ^{237}Pu, have been used, which allow experiments at very low concentrations (8.4 x 10^{-11} M and 3.7 x 10^{-11} M, respectively), close to the actinide concentrations expected in the environment. In these experiments, humic acid (HA) was used as a competing ligand. Humic acids are an important ligand, significantly affecting the sorption and mobility behaviour of actinides in the environment. Humics, polyelectrolyte organic macromolecules, are ubiquitous in natural aquifers, with concentrations in groundwater estimated to range from less than a 1 mg·L^{-1} to more than 100 mg·L^{-1}. Humics bind virtually all metal ions, affect strongly the speciation and transport of radionuclides, including actinide elements, and are one of the most important environmental ligands. The humic acid was chosen because it is a strong competing ligand and because it is possible that bentonite colloids in the envieoment might encounter it, and so the competition between bentonite and humic acid is of interest, beyond the rate of dissociation from the bentonite.

3.1.1   Materials and Methods

Commercially available humic acid from the Aldrich Chemical Company (Germany) was used in the experiments in sodium form. Natural bentonite from the Aldrich Chemical Company was purchased and used without any further pre-treatment. The bentonite specific surface area was found to be 30.98 m²·g^{-1} and the bulk density is 1.85 g·cm^{-3} (Mihoubi and Bellagi, 2006). The point of zero charge of bentonite is reported to be at pH=7.8 ± 0.1 (Yu et al, 2006).

^{237}U and ^{237}Pu production and purification
^{237}U ($T_{1/2}$ = 6.75 d, Eγ = 59.54 keV (34.5 %); 208.00 keV (21.2 %)) with high specific activity was produced by the ^{238}U (γ, n) ^{237}U reaction on the MT-25 electron accelerator (FLNR-JINR, Dubna, Russia). A target, containing 11 mg of natural UO$_2$(NO$_3$)$_2$ was irradiated for 5 h with 25 MeV gamma rays, yielding 49.5 MBq per mg ^{238}U. After cooling the target for several hours to reduce the activity of the short-lived fission and activation products, radiochemical separation and

purification of [237]U was carried out by recoil nuclei collection on MnO_2. The final purification and concentration of [237]U radiotracer was carried out by ion-exchange chromatography on a 50x2 mm column loaded with Dowex 1x8 (mesh 200-400) anion exchange resin from a 10% solution of 9 M HCl in ethanol. After rinsing with 1 mL of the same solution, the [237]U was eluted with 1 M HNO_3 (Suprapur, Merck). The 1 mL stock solution, containing 1.3 MBq [237]U, was prepared with dilute HNO_3 (Suprapure, Merck). It was stored in a 2 mL Eppendorf tube and 10 μL added as needed to each 5 mL batch sample to reach a [237]U activity level of 2.6 kBq mL^{-1}. The overall uranium concentration was approximately 8.4×10^{-11} M, which in fact represents the molarity of [238]U, while the [237]U concentration in the samples was more than an order of magnitude lower (3.6×10^{-12} M).

[237]Pu ($T_{1/2}$ = 45.3 d, Eγ = 97.1 keV (12.5%), 101.1 keV (20.1%), 113.9 keV (7.6%)) was produced by the $^{235}U(^{4}He,2n)^{237}Pu$ reaction. In this case, since the product is a different element, the separation was straightforward. As part of the separation procedure following the production of [237]Pu, the plutonium is produced in the Pu(III) oxidation state by elution with HCl 9 M/NH_4I 0.1 M.

Batch Sorption Experiments

A series of batch experiments were performed at room temperature and ambient atmosphere ($pCO_2 = 10^{-3.5}$ atm) in order to study the effect of humic acid on uranyl sorption on bentonite. In all experiments the solid to solution ratio was 1 g L^{-1}. The amounts of humic acid and U adsorbed onto bentonite were determined from the difference between the concentrations in the suspension and supernatant after the equilibration time. The solutions were adjusted to the required pH by adding appropriate quantities of freshly prepared diluted solutions of KOH (Merck) or HNO_3 (Suprapure, Merck). In all experiments the ionic strength was maintained at the necessary value using $NaClO_4$. After several hours the pH of the solution was checked again, a correction made if needed, and the sample spiked with the [237]U or [237]Pu stock solution. The final concentrations of uranium or plutonium in the solution were approximately $2.6x10^{-10}$ and $3.7x10^{-11}$ M, respectively. The polypropylene tubes were shaken from time to time. After 5 days, the supernatant was separated by centrifugation at 4000 rpm for 10 min and a 1 mL aliquot was taken to determine the activity of [237]U. The concentration of humic acid in the supernatant was determined by UV spectrometry using a T-60 UV-VIS spectrophotometer (PG Instruments), measuring the absorbance at 253 nm. The [237]U and [237]Pu analytical concentrations were measured by γ- spectrometry, counting the activity of 1 mL aliquots on a HPGe detector GC2520 (Canberra Ind.) with relative efficiency 25% and resolution FWHM= 0.9 keV for 122 keV and Genie-2000TM software (Canberra Packard).

The concentration of natural U in the higher concentration samples was determined by LSC on a Wallac Quantulus 1220 ultra low level LSC spectrometer using 20 mL polyethylene vials and OptiPhase HiSafe 3 cocktail (Perkin Elmer). A set of preliminary experiments was carried out to examine humic acid sorption on the tube walls, and no evidence for significant sorption or precipitation during the centrifugation was found. U and Pu sorption on vial walls was studied at moderate pH and was found to be negligible. In all figures, the error bars represent the standard deviation of three experimental points.

3.1.2 Results and discussion

Examples of the results are described below: more details are given in Ivanov et al (2012).

Uptake of U(VI) and humic acid by bentonite

Uranyl sorption on 1g L^{-1} bentonite was studied as a function of pH at ionic strength 0.01 M both in the absence and presence of HA, and the results are given in Figure 3. U(VI) sorption in the absence of HA was found to be strongly pH dependent. At pH lower than 3.1, U(VI) retention on bentonite is negligible, then it increases sharply with increasing pH, and a distinct sorption edge was found at relatively low pH, within a narrow range between pH 3.1 and 4.5. Maximum sorption

of U(VI) on 1g L^{-1} bentonite (80-90 %) was found to take place at pH 4 – 6. Further increase in pH results in a gradual decrease of sorption from 80 % at pH 6 to approximately 20 % at pH 9.
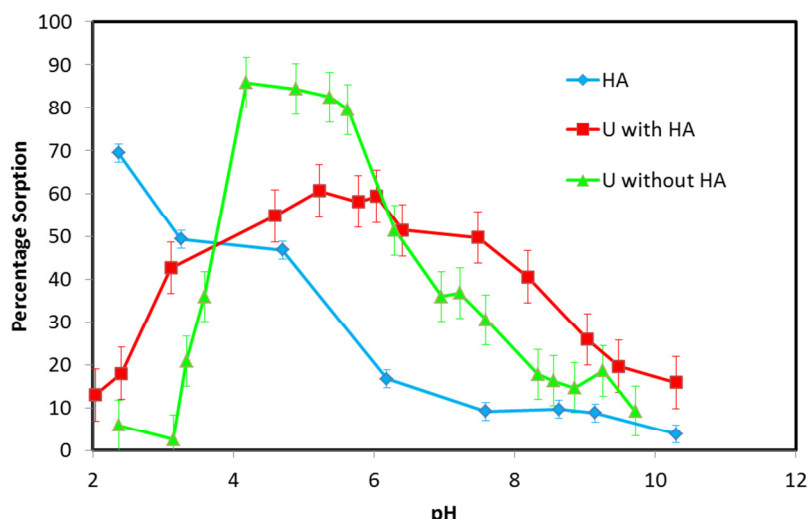

Figure 3: Sorption of uranyl and humic acid on bentonite as a function of pH.

In the presence of humic acid, the uranyl uptake by bentonite is significantly modified. The sorption of humic acid on bentonite was also studied and the general trend is of decreasing uptake with increasing pH. At pH higher than 7.8 (pHpzc of bentonite), the uptake is negligible, due to the electrostatic repulsion between the negatively charged humic acid and the charged bentonite surface. Compared to humic acid sorption, the retention of U(VI) in the presence of humic acid is more complex, however at pH higher than 6.0 the general trend is the same, decreasing with increasing pH. At low pH (below 3.8), the addition of HA enhances U(VI) sorption compared to the HA-free system which indicates that in the acidic pH range, the uranium distribution is strongly influenced by complexation with humic acid sorbed onto bentonite (ternary surface complex formation). While in the absence of HA the prevalent uranium species at low pH is UO_2^{2+}, in the presence of humics the U(VI) speciation at this pH range is dominated by the uranyl-humato complex UO_2HA (Ivanov et al 2012), which similarly to HA is expected to be readily sorbed on bentonite at low pH.

In the range between pH 3.8 and 6.5 the sorption of U(VI) is significantly reduced in the presence of humics, compared to the binary U(VI)-bentonite system and approximately 55 – 60 % of uranium is bound to the solid phase. In this pH range, the dominant uranyl species are uranyl-humic complex UO_2HA and the uranyl mono hydroxo humate complex $UO_2(OH)HA$ (Ivanov et al, 2012). Taking into account that HA sorption on bentonite drops from 50 to less than 20% within this pH range, the reduced sorption of uranium in the presence of HA seems reasonable. At pH between 7 and 9 the uranyl uptake is slightly enhanced in the presence of HA compared to the retention on bentonite in the absence of humics.

At high pH, the uranium sorption is less sensitive to the presence of humic, compared to the near-neutral pH area, probably because at this HA concentration the humic does not compete effectively with carbonate for the uranyl complexation. At high pH, the U(VI) speciation is dominated by the uranyl carbonate complexes, and at pH>8.5 the uranyl tri-carbonato complex $[UO_2(CO_3)_3]^{4-}$ becomes the dominant species (Ivanov et al 2012).

The sorption of U(VI) at a concentration of 10^{-4} M on bentonite in the presence of humics was also studied and the experimental results are also given in Figure 3. The uranyl sorption at high concentration level shows significant differences, compared to the lower concentration level uranium ternary system, especially in the alkaline area. In the low and near-neutral pH range, the sorption behaviour appears to be similar for the two uranium concentrations. However, at high pH there is a significant difference, and U(VI) at the higher concentration shows much higher

sorption. This result shows the importance of studying systems at concentrations expected in the environment.

Reversibility in U(VI)/Pu(III) – bentonite – humic ternary systems
The effect of the addition order of ternary system components was investigated at pH = 5.0 and ionic strength 0.01, and the results are given in Figure 4. Three different experiments are shown in Figure 4: in the first, the uranyl and humic were allowed to interact prior to contact with the bentonite, whilst in the other experiments, the uranyl was allowed to associate with the bentonite for 1 and 7 days prior to the introduction of the humic. The kinetics of uranyl distribution between the supernatant and the solid phase was found to be relatively slow and approximately four days were required to reach equilibrium, which appears to be between 50 and 60 % adsorbed in the presence of HA. In the U(VI)-bentonite binary systems (before addition of HA) the initial sorption step is significantly faster, compared to the ternary humic systems, and it takes approximately 1 h to reach the point of 50% sorption.

As seen in Figure 4, the equilibrium value of 80 – 85 % retention in the binary U(VI) – bentonite system is eventually reached and the amount of U(VI) adsorbed on bentonite remained stable until the humic acid was added to the sample. Following addition of the humic, there is a decrease in the amount of Eu bound to the bentonite. No significant effect of the addition order and pre-equilibration time was observed in this experiment beyond 2 days. Therefore, the interaction of uranyl with bulk bentonite appears to be reversible.
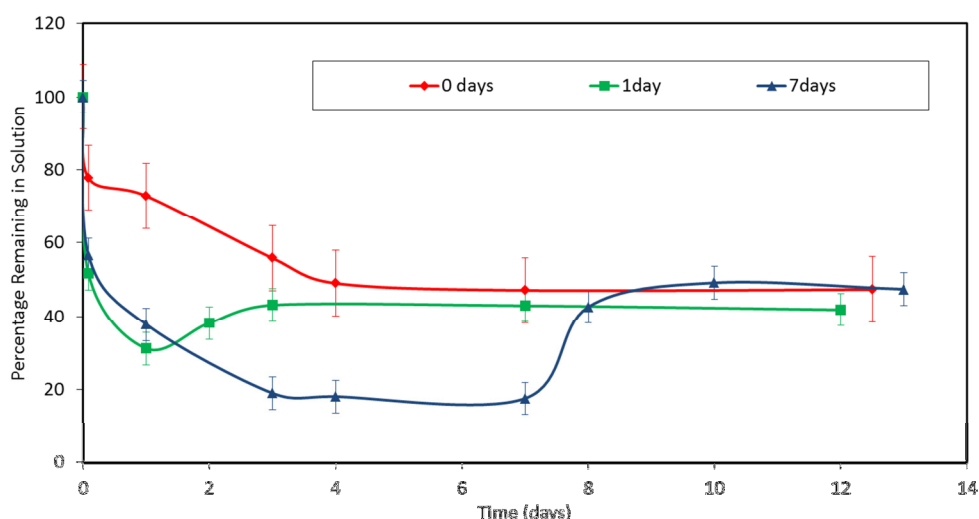

Figure 4: Effect of addition order in the U(VI)-bentonite-humic acid ternary system.

Figure 5 shows the results of an equivalent set of experiments to those in Figure 4, but using [237]Pu instead of [237]U. This time, the [237]Pu was added as Pu(III). For the system where metal ion and humic were mixed prior to contact with the mineral phase, there is a rapid, initial increase, as for the U system, but whereas the U data show equilibrium after a few days, this time the amount bound continues to increase , and the system has not reached equilibrium even after 25 days. Hence, unlike uranyl the interaction of trivalent actinide ions with bentonite is not instantaneously reversible.
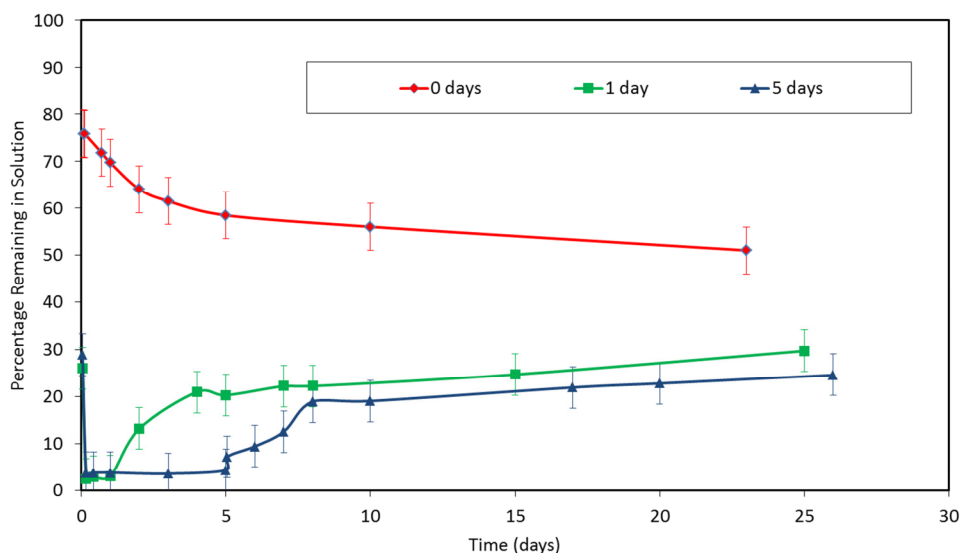
Figure 5: Effect of addition order in the Pu(III)-bentonite-humic acid ternary system.

3.2 Eu/Bentonite ternary systems

The authors involved in the work in this section are: N. Sherriff, R. Issa and N.D. Bryan (*Centre for Radiochemistry Research, School of Chemistry, University of Manchester, Manchester, U.K.*).

In these experiments, the interaction of europium with bentonite has been studied. In initial experiments, humic acid was used as a competing ligand. Later, EDTA was used as an alternative for the calculation of first order bentonite dissociation rate constants.

3.2.1 Materials and Methods

The clay used in this work is Wyoming bentonite, which is a 'sodium bentonite'.

Bulk humic acid and Eu uptake experiments

9 ml of each of the humic acid solutions (10, 20, 50 & 100 ppm) were transferred to 10 ml plastic tubes, and then 1 ml of sodium perchlorate solution (1.0 M) was added to each tube. The pH was adjusted to pH = 6.0 ± 0.1, using either 0.1 M or 0.01 M HCl or NaOH solutions, as required. The pH-meter used was an Orion model 720, together with a BDH double junction glass electrode. UV/VIS spectra were recorded for the samples using a UV-Visible spectrophotometer (type T60 with UVWin5 software v5.50.5), using 2.5 ml aliquots from each sample, (day 0 sample). The UV/VIS spectra were recorded between 200 and 700 nm. The aliquots were returned to the original mixtures, and then 0.05 g ± 0.0005 g bentonite was added to each tube. For analysis, the samples were centrifuged for 20 minutes at 3500 rpm, using a MSE 3000i model centrifuge. The centrifuging was repeated for some samples when necessary (especially for 10 ppm HA solutions). The samples were measured again by UV-Visible spectrophotometry (day 1). After analysis, the aliquots were returned to the tubes and the solid was re-suspended. The systems were then kept, while they were measured regularly by UV-Visible spectrophotometry, using the same procedure.

Experiments to study the uptake of Eu in the presence and absence of humic acid were conducted in a similar way, except that 1.333 ml of ^{152}Eu, 1 kBq ml^{-1}, 1 ml of 1 M NaClO$_4$, 7.667 ml of humic acid solution were mixed in 10 ml polyethylene tubes. The pH was accurately adjusted to 6.0 +/- 0.1, using either 0.01, 0.10 M HCl or NaOH solutions, as required. 1.5 ml aliquots in 25 ml plastic tubes were measured with gamma spectrometry (day 0). The aliquots were returned to the original solutions and 0.05 g of bentonite was then added to each tube. The pH was adjusted again. For analysis, the samples were centrifuged at 3500 rpm for 20 minutes, and 1.5 ml aliquots

were measured again with a gamma-ray spectrometer (day 1). The aliquots were returned again to the original solutions, which were re-suspended and kept, while they were measured (30 days).

Preliminary dissociation experiments

Preliminary experiments had to be performed to establish what quantities of materials would be used for the batch dissociation experiments. Preliminary sorption experiments were performed with [152]Eu (1 ml, 1 kBq), deionised water (8 ml) and $NaClO_4$ (1 ml), to this was added bentonite clay (0.05 g, 0.1 g and 0.5 g). The samples were adjusted to pH 7 ($\pm$ 0.1). They were left on a slow rocker for 68 hrs before centrifugation (10 ml, 4000 rpm, 15 mins followed by 2 ml, 14000 rpm 35 mins) and analysis on the gamma ray detector to determine the amount of bentonite clay required to remove nearly 100% of the [152]Eu from the solution.

Preliminary dissociation experiments were then performed using [152]Eu (1 ml, 1 kBq), deionised water (8 ml) and $NaClO_4$ (1 ml). EDTA was added (0.1 M, 0.01 M, 1×10^{-3} M and 1×10^{-4} M) and the pH adjusted to 7 ($\pm$ 0.1). Following addition of EDTA, bentonite (0.5 g) was added. The samples were left on a slow rocker for 18 hrs. Centrifugation (10 ml, 4000 rpm, 15 mins followed by 2 ml, 14000 rpm 35 mins) was performed and the solution was analysed by gamma ray spectrometry to determine the amount of EDTA required to retain nearly 100% of [152]Eu from the bentonite.

Bulk dissociation experiments

Bentonite clay (0.5 g) was added to a tube with deionised water (8 ml) $NaClO_4$ (1 ml, 0.1 M) and [152]Eu (1 ml, 1 kBq), the system was then adjusted to pH 7 ($\pm$0.1). 30 tubes were prepared in this way to give 10 analysis opportunities (triplicates). The tubes had the clay suspended (maximising contact with the Eu(III)) and were left on their sides, maximising contact between dissolved species and the clay. As all of these tubes were spiked with Eu(III) at the same time. The contact time between the Eu(III) and the bentonite was controlled by the addition time of the EDTA. Before the addition of EDTA, the tubes were centrifuged on a BOECO C-28A centrifuge (15 mins, 4000rpm) to remove particles larger than 2 μm. Once this was complete, the top 4 ml of suspension in the tube was removed and distributed into 2 ml cuvettes. These were then centrifuged on the SIGMA micro-centrifuge (35 minutes, 14000 rpm): this removes all particles larger than 0.25μm. Following centrifugation, 1 ml of the solution was removed and replaced by EDTA (1 ml, 0.1 M), which when introduced to the 10 ml system gave an overall EDTA concentration of 0.01 M. Once the EDTA was added, the tubes were rocked for 1 hour to re-suspend the clay. Following the re-suspension, the tubes were again centrifuged as before and 1.5 ml was removed for analysis by gamma ray spectrometry to measure how much of the Eu(III) was clay bound, and how much was in solution. Due to the non-destructive nature of gamma ray spectrometry, upon completion the aliquot can be returned to the sample tube, the clay re-suspended and the sample put away for later analysis.

Colloid studies

The experimental techniques have been adapted from Bouby et al (2011). The clay was sieved to <63 mm. Two separate 10 g fractions were measured and placed in large beakers. Two techniques were used to generate bentonite colloids: using LiCl a delaminated suspension can be produced; or using deionised water a non-delaminated suspension can be created.

Delaminated Samples (Suspension 1)

10 g of bentonite clay was soaked in 1 L LiCl (1 M) for 10 days, and the beaker was covered in protective foil to ensure no contamination and also to ensure no loss of water through evaporation. To aid the generation of colloids, through abrasion, the suspension was kept stirring through the entire 10 days. The resulting bentonite slurry was evenly distributed into centrifuge tubes (50 ml x 20), even slurry distribution was achieved by keeping the slurry stirring and extracting the required 50 ml using a syringe. Each tube was centrifuged (4000 rpm, 11 minutes); this was calculated to ensure no bentonite colloids remaining in solution were larger than 500 nm. Each tube had the supernatant fluid decanted, and was then refilled to the 50 ml mark with deionised water and sonicated in a sonic bath for 10 minutes to re-suspend the clay. This process

of centrifugation and sonication was repeated a further 3 times. The supernatant fluid remaining after the 4th centrifugation step constituted the colloidal stock, which was stored in the dark.

Non-delaminated Samples (Suspension 2)

This suspension was created in much the same way as the first, but did not have the LiCl step included. The clay was allowed to equilibrate with deionised water over a 10 day period with stirring. The method then followed the same centrifugation/re-suspension techniques as for the delaminated sample.

Concentration determination

ICP-AES (Inductively coupled plasma atomic emission spectroscopy) was used to measure the concentration of the colloids. Each sample was diluted with deionised water (1 ml sample, 9 ml deionised water), and to this HNO_3 was added (0.2 ml) prior to analysis to determine the concentrations of Al and Mg (method adapted from Laaksoharju, 2005).

Ultrafiltration

Ultrafiltration was performed on the colloidal stock to assess the sizes of the colloid. The ultrafiltration was performed under pressure (argon, 1.5 bar) to push solution samples through an ultrafiltration filter. The filters were composed of PES (polyethersulfone). SEM-EDX (Scanning electron microscopy with energy dispersive x-ray spectroscopy) was used to analyse the first filter paper from the ultrafiltration (300 kDa). The aim was to determine if colloids could be seen, and also to confirm that any colloids on the filter had compositions typical of bentonite using EDX data. SEM-EDX was performed in the School of Earth, Atmospheric and Environmental Science, using a Philips XL30 FEG ESEM with an EDX module.

^{152}Eu binding to bentonite colloids

Eu(III) was added to the bentonite stock solution to test if any uptake could be detected. Bentonite colloid stock (3.5 ml) and ^{152}Eu (3.5 ml, 35 kBq) were added together, and the pH was adjusted to 7 ($\pm$0.1). This suspension was left for 68 hrs to equilibrate. Simultaneously, the filters (300, 10 and 3 kDa) were pre-treated with 10^{-4} M $Eu(NO_3)_3$ solution to bind Eu(III) to any binding sites on the membranes before the filtration commenced. This pre-treatment stops any ^{152}Eu(III) in the sample solutions from binding to the filter itself, as the binding sites are already occupied by the stable europium (Pitois et al, 2008). The solutions were filtered sequentially through each of the membranes. The filtering experiments were performed in triplicate.

The sample activity was analysed using a semi-conductor high purity germanium detector (121 KeV). 1.5 ml of sample was measured for 1200 s. All samples used the same volume of solution, the same size container and the same sample container position, so that the results can be compared accurately.

3.2.2   Results

Humic Acid Sorption

Interaction of humic acid with bentonite was studied to allow the competition experiments to be interpreted. Figure 6 shows the uptake of humic acid onto bentonite.

The uptake of humic acid is relatively rapid, with sorption apparently complete by 2 days. The fraction of the humic acid that is sorbed to the bentonite shows only a small decrease with increasing humic acid concentration. In the 10 ppm system, the extent of sorption is approximately 85%, whilst at 100 ppm, it is still 80%.

Eu uptake to bentonite

The uptake of Eu to bentonite as a function of humic acid concentration is shown in Figure 7. The data are plotted as C/Co, where C is the concentration of Eu remaining in solution at any given

time, and Co is the initial concentration of Eu in the system before sorption starts (in this case 7.91×10^{-10} M).
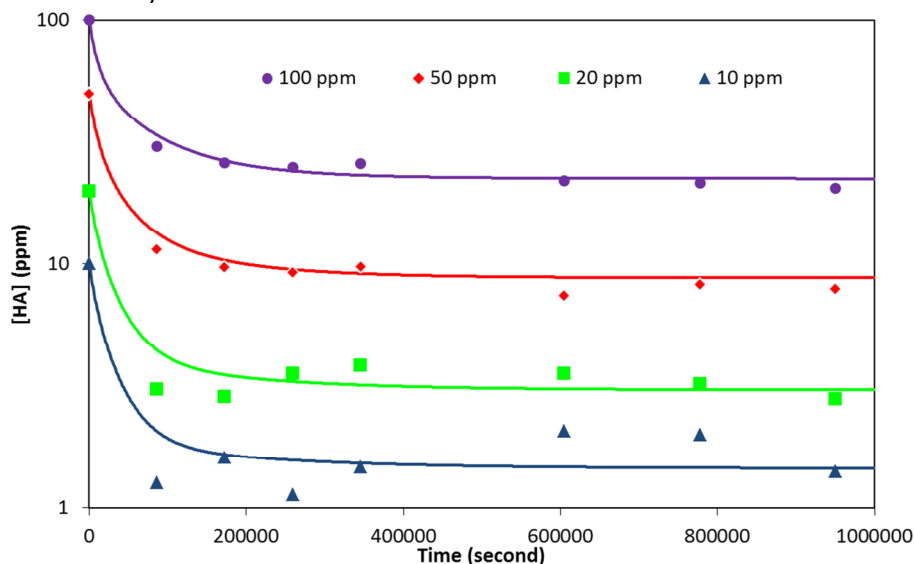

Figure 6: Sorption of humic acid to bentonite, as a function of humic acid concentration.

The sorption of Eu(III) in the presence and absence of humic acid is shown in Figure 7. The data shown in the figure are for experiments where the Eu was pre-equilibrated with the humic acid before contact with the bentonite. Therefore, the time series data in this figure provide no information on the kinetics of bentonite dissociation. There is evidence of slow Eu uptake kinetics in all of the systems, even in the absence of humic acid, and it takes 14 days before an apparent steady state concentration of Eu is remaining in solution. The slow kinetics in the systems containing humic acid could be due to the slow formation of humic ternary complexes. However, those in the HA-free system must idicate a slow component to the interaction of Eu(III) with bentonite, the increase in the amount of Eu bound is approximately 2.5% in the HA-free system between 1 and 14 days. This seems small, but it corresponds to an increase in K_d by a factor of approximately 4 (decrease in percentage Eu free in solution from 3.6 % to 0.97 %), and so there is an increase is effecive binding strength.

Beyond the kinetics, the most interesting result in Figure 7 is that the behaviour of the Eu seems independent of humic acid for humic concentrations of 20 ppm or below, which suggests that at the concentrations of humic typically found in groundwaters, there will be no effect on the solid/solution partition.
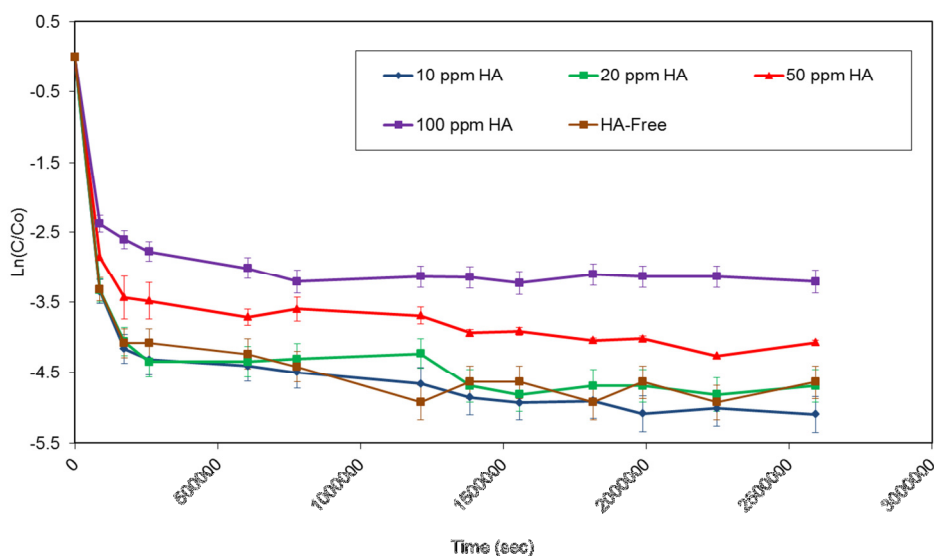

Figure 7: Sorption of Eu to bentonite, as a function of humic acid concentration.

17

Model of Uptake of Eu on Bentonite in Presence of Humic Acid

A mathematical model to describe the uptake of humic acid and Eu(III) on bentonite was developed. Humic ternary systems are prone to complex behaviour (Bryan et al 2012). The interaction of humic acid and radionuclides has been studied recently, and a model has been developed that can predict the binary interaction between metal ions and humics (e.g., Bryan et al. 2007; King et al., 2001). Further, there are models that can predict the interactions of humics with mineral surfaces (Bryan et al, 2012). However, the prediction of the speciation of the metal ion in the full ternary system is very difficult, because the sorption of metal ion-humic acid complexes is not sufficiently understood, and because humic acids are in fact complex, heterogeneous mixtures (Bryan et al, 2012). Further, it is known that in humic ternary systems, chemical fractionation can take place, which is where sorption to a surface takes place and the chemical species in solution can have different binding strengths to those sorbed onto the solid phase. In such systems, there is a need to define more than one type of humic acid. It is also known that the different fractions of humic acid can have very different interactions with inorganic surfaces (e.g. Van de Weerd et al 2001). Attempts were made to model the behaviour in Figures 6 and 7 with models that had:

- 1 type of humic and 2 bentonite surface binding sites (Model 1);
- 2 types of humic and 1 bentonite surface binding site (Model 2).

Such models have been applied previously to quartz sand and iron oxide ternary systems with some success (e.g. Bryan et al, 2012). However, it was found that the models were unable to simulate the data, and a model with:

- 2 types of humic and 2 bentonite surface binding sites (Model 3)

was required to simulate the data. The system of equations used to model the data in this model are shown in Figure 8.
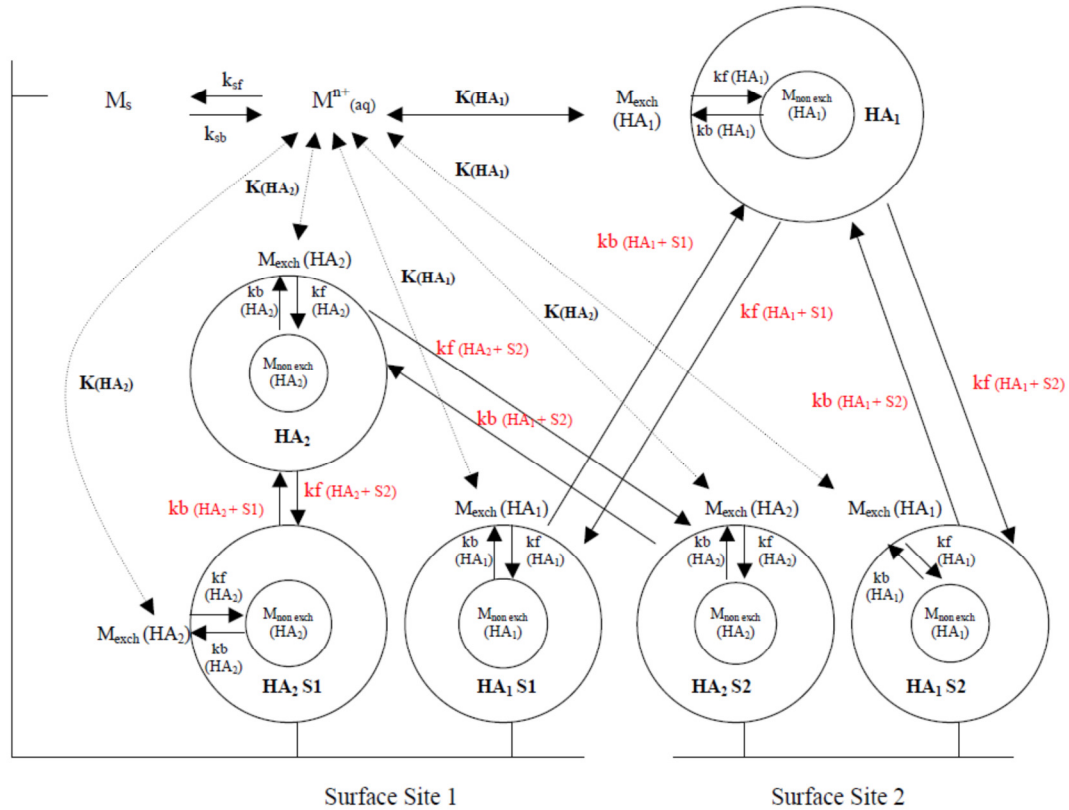

Figure 8: System of processes used in humic ternary system model; $\leftrightarrow$ and $\rightleftharpoons$ represent processes described with equilibria and slow reactions, respectively (full details in Appendix A)

The fits to the experiments are given as the lines in Figures 6 and 9. The fit to the humic sorption data is relatively good (Figure 6). However, the fit to the Eu data is less good. The 2 humic/2 site model allows the fitting of the equilibrium uptake of the Eu by the bentonite in the presence of the humic. However, it is unable to fit the Eu kinetics.

The principal objective of this work is to study the dissociation behaviour of radionuclides from bentonite. Figure 8 shows that the humic acid introduces considerable complexity to the system, because it is a complex mixture and because the humic itself introduces complex kinetics into the system. The interaction of the humic with the metal has a kinetic component and all four equations describing the sorption of the humic require a kinetic description. It became obvious at this point that although humic acid can provide useful information, and it can be used to show whether or not the interaction of a radionuclide with bentonite is reversible, its behaviour is too complex to allow calculation of bentonite dissociation rate constants, because that would require deconvolution of the humic and bentonite kinetics. Further details of the humic ternary system model are given in Appendix A.
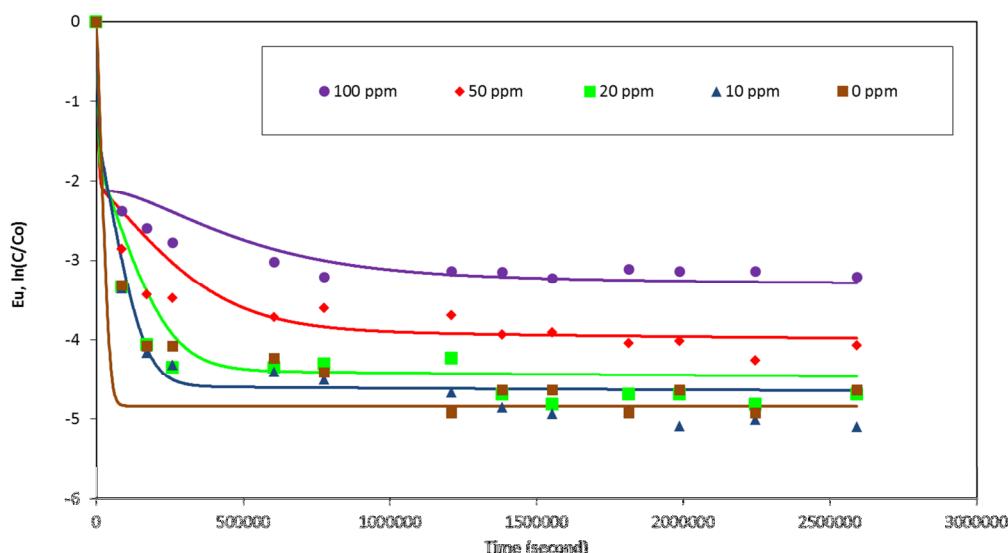

Figure 9: Model fit to Eu kinetic uptake data as a function of humic acid concentration.

Eu Dissociation from bentonite

Preliminary investigation

Preliminary experiments were performed using different quantities of bentonite clay to explore Eu(III) binding affinity. Table 1 shows the results of these preliminary experiments. After several experiments, it was determined that 0.5 g of bentonite in a 10 ml suspension of NaClO$_4$ (0.1 M, 1 ml), deionised water (8 ml) and ^{152}Eu(III) (1ml, 1kBq) was the optimum amount to bind all of the Eu(III). EDTA was chosen as the competing ligand that would remove the Eu(III) from the clay, since it has a high affinity for Eu(III).

Table 1: Eu(III) sorption for different quantities of bentonite clay.

Bentonite (g)	Eu(III) sorbed (%)
0.05	72.9
0.1	64.1
0.5	96.3

Table 2: Eu(III) retained in solution by EDTA

EDTA (M)	Eu(III) retained in solution (%)
0.1	100
0.01	100
1x10^{-3}	33.6
1x10^{-4}	6.2

Different concentrations of EDTA were added to the systems before contact with bentonite to establish the concentration that would retain 100% of Eu(III) from the bentonite. Table 2 shows the results of these preliminary experiments. After the experiments, it was decided that 0.01M EDTA was the optimum concentration for this system.

Eu(III) batch dissociation experiments

These batch experiments have been on-going since November 2012. So far, triplicate experiments have been started after 1, 7, 21, 65 and 115 days of Eu(III)/bentonite clay interaction, prior to the addition of EDTA. Figure 10 shows the dissociation of Eu(III) from bentonite over time.
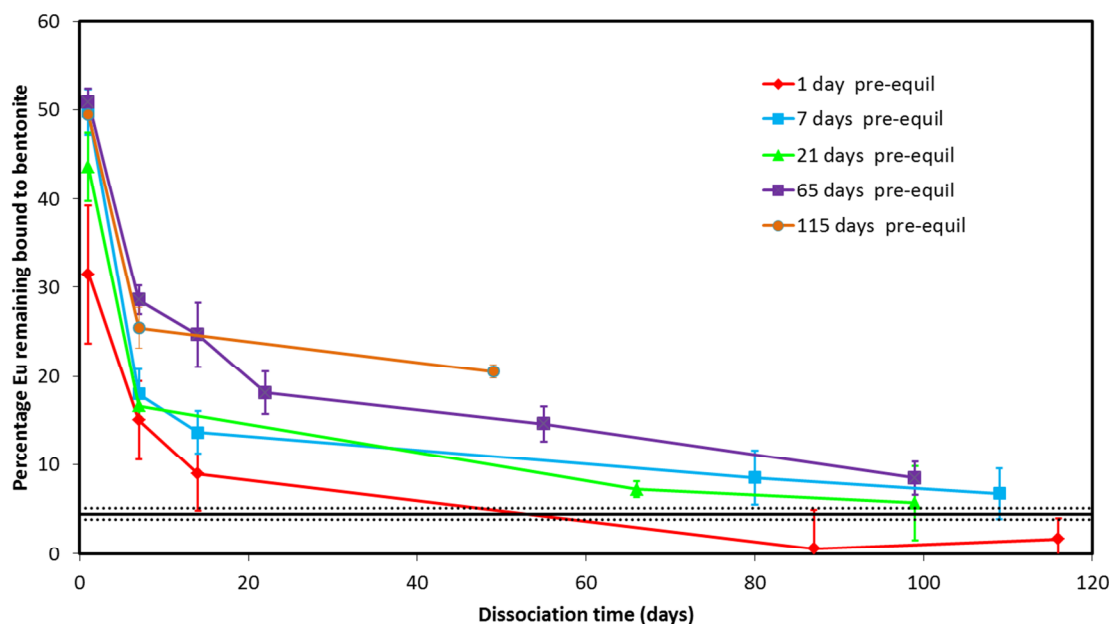

Figure 10: Eu(III) dissociation from bentonite clay versus time in contact with EDTA as a function of Eu/bentonite pre-equilibration time.

From Figure 10, it can be seen that the Eu(III) dissociation from bentonite upon the addition of EDTA follows a similar pattern for all of the pre-equilibration times. A large part of the Eu(III) (30-50%) dissociates almost instantaneously from the clay, and the rest dissociates over time. Whilst there are insufficient data to conclude definitely that pre-equilibration can increase the amount that dissociates slowly, there are some interesting differences.

On the first day of contact time for all 5 samples, approximately 50% of the radionuclide is removed from the clay (the first sample has a value of 31 % of Eu(III) remaining on the bentonite, but has a large error ($\pm$ 7.5%). Analysis on day 7 however shows some differences. For pre-equilibration times of 1, 7 and 21 days, after 7 days contact with EDTA, the amount of Eu(III) bentonite bound is approximately 16.6% ($\pm$ 3.0%). For pre-equilibration times of 65 and 115 days, after 7 days EDTA contact the amount of Eu(III) bentonite bound is approximately 27% ($\pm$ 4.4%).

Rate constants
Figure 11 shows the raw data from Figure 10, but this time plotted as the natural logarithm of the percentage of Eu bound to bentonite versus EDTA contact time. The advantage of a plot such as this, is that any portions of the dissociation that occur with a single first order dissociation rate constant will appear as a straight line in Figure 11, and the rate constant may be determined from the gradient. There are several interesting points to note. First, the systems with pre-equilibration times greater than 1 day show different behaviour to that of the 1 day system. For the shortest pre-equilibration time, the dissociation is distinctly faster, with a smaller decrease in gradient as EDTA contact time progresses, compared to the other systems. The average dissociation rate

constant for this system (taken from day 1 of EDTA contact until the system reaches apparent equilibrium) is approximately 10^{-6} s^{-1}.
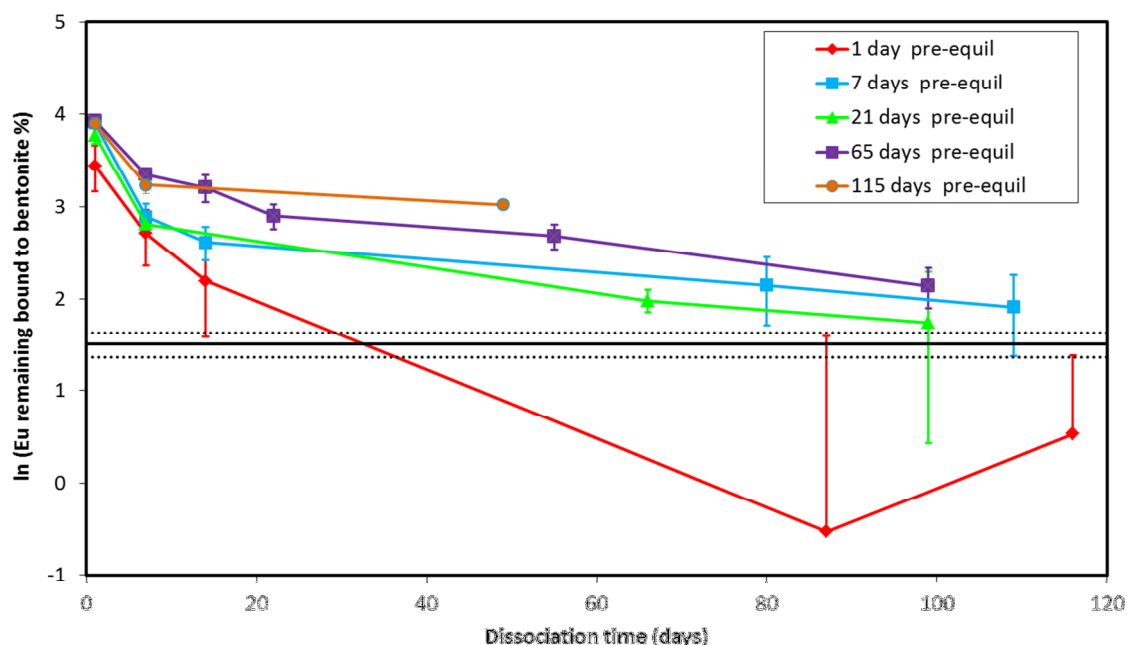

Figure 11: natural log plot of bentonite dissociation experiment: ln(percentage bound to bentonite) vs EDTA contact times, as a function of pre-equilibration time.

For the longer pre-equilibration times, each of the plots shows more than one gradient. There is faster dissociation at the start of the experiment, but after approximately 7 days EDTA contact, there is a distinct reduction in reaction rate. More than this, the plots appear to have similar rates of decrease beyond 7 days EDTA contact. First order dissociation rate constants were calculated by regression for these portions of the plots using the data from Figure 11, and the results are shown in Table 3. The regression also provides the fraction of the bound Eu that is contained in this most slowly dissociating fraction, and these data are also given in the table. Note, for the system with a pre-equilibration time of 115 days, there are currently only two data points in the region of slow dissociation, and so there will be large uncertainties associated with the values of the rate constant and amount for this system.

Table 3: Dissociation rate constants, reaction half time data and amounts for the most slowly dissociating fraction. Note, calculating an overall rate for all data in Figure 11 gives first order constants in the range $2.0 +/- 0.5 \times 10^{-7}$ s^{-1} for all systems.

Pre-equilibration Time	Dissociation rate constant (s^{-1})	Amount of Eu in fraction (%)	τ (Days)
Day 7	1.01×10^{-7} ($\pm 3.11 \times 10^{-8}$)	17.0 ($\pm$ 3)	79
Day 21	1.38×10^{-7} ($\pm 1.32 \times 10^{-7}$)	17.5 ($\pm$ 10)	58
Day 65	1.42×10^{-7} ($\pm 2.83 \times 10^{-8}$)	28.2 ($\pm$ 3.5)	57
Day 115	5.90×10^{-8} (Insufficient data for error)	26.4	137

Colloid Systems

Using the formula and the quantity of each element detected, a concentration for the bentonite colloids can be calculated. Table 4 shows the calculated bentonite concentrations in the two suspensions.

Table 4: calculated concentrations of bentonite colloids

Delaminated

Element used for calculation	Bentonite concentration / ppm
Al	222
Mg	214

Non-delaminated

Element used for calculation	Bentonite concentration / ppm
Al	251
Mg	219

Taking the average of both calculated concentrations in Table 4 gives the bentonite concentrations of the stock solutions, which are 218 ppm for the delaminated sample and 235 ppm for the non-delaminated solution.

Colloid ultrafiltration

Using delaminated colloid solution, ultrafiltration was performed using filters of 300 kDa, 10 kDa and 3 kDa cut-off to measure the concentration of colloids within those size ranges. Although the relationship between size and nominal molecular weight cut-off is complex, an estimation can be made:

- The 300 kDa – 10 kDa fraction will contain particles no larger than *ca.* 20nm;
- the 10 kDa – 3 kDa fraction will contain particles no larger than *ca.* 2nm;
- the <3 kDa fraction will contain particles no larger than *ca.* 1nm.

The results of the ultrafiltration are shown in Table 5.

Table 5: Results from ultrafiltration of delaminated colloid stock solution

Fraction size / kDa	Bentonite concentration / ppm
Stock (whole sample)	218
300 - 10	2.96
10 - 3	0.87
< 3	N/A (element ratio does not match)

Out of the total colloid concentration, only 1.76% makes it through the first filter. This suggests that over 98% of the colloids in the suspension must be above 20 nm in size. Most of the colloids that do pass the first filter are in the 300 – 10 kDa fraction, and have a size range of approximately 2 – 20 nm and constitute 1.36 % of the total concentration, whilst a very small amount (0.40 %) are in the 10 – 3 kDa fraction with a size range of approximately 1 – 2 nm. The ICP results for the <3 kDa fraction showed an Al : Mg ratio of 2.7:1. Hence, it seems that the Al and Mg within this fraction are not bentonite colloids. The material in this fraction is smaller than 1 nm, which is the lower limit of the colloid size range, and so we would expect these concentrations to represent the Al and Mg concentrations in the true solution. The colloid concentrations in the fractions are illustrated in Figure 12.
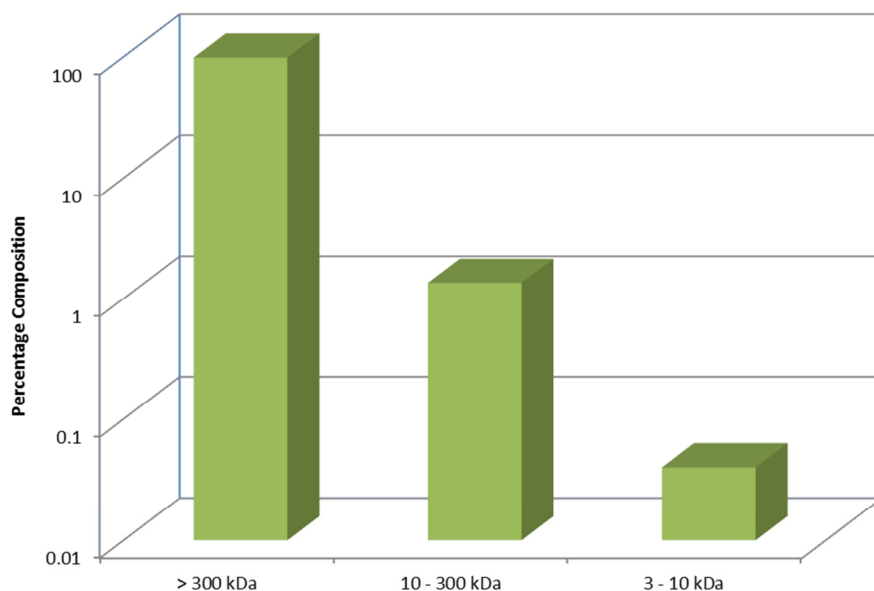
Figure 12: colloid concentration for each fraction size

Eu binding to bentonite colloids

Table 7 shows the results of the Eu ultrafiltration experiments.

Table 7: Eu activity results from ultrafiltration sampling determined from triplicate experiments

Fraction size (kDa)	% Eu in fraction	2 sigma error
> 300	99.1	1.1
300 > 10	0.78	1.08
10 > 3	0.11	0.06
> 3	0.06	0.05

Most of the radionuclide does not pass the first filter. In fact 99% of the [152]Eu(III) fails to make it through the first filter of 300 kDa. Figure 13 shows the Eu concentration in the size fractions, compared to the concentrations of the colloids in the same fractions. There is a good correlation between the colloid and Eu data.
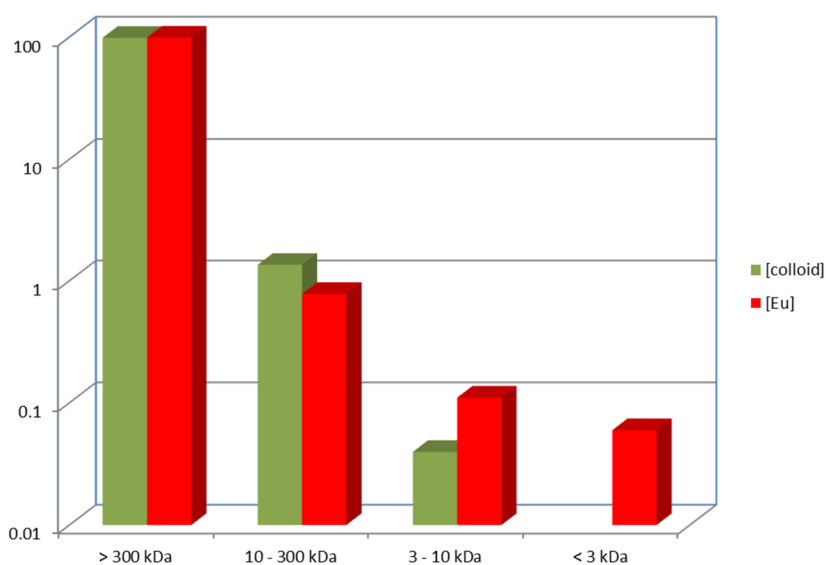

Figure 13: the colloid and [152]Eu(III) concentrations for each size fraction.

3.3 ^{232}U/^{228}Th Experiments

The authors involved in the work in this section are: N. Sherriff and N.D. Bryan (*Centre for Radiochemistry Research, School of Chemistry, University of Manchester, Manchester, U.K.*).

At the time of writing this report, experiments are underway to extend the work with Eu described in Section 3.2 to systems of ^{232}U and ^{228}Th. ^{228}Th is the daughter isotope of ^{232}U. The first step is to separate the ^{228}Th (and subsequent daughters) from the ^{232}U.

The separation of ^{232}U from its daughters was carried out with an ion exchange method. A 0.7 x 10 cm column packed with 100 mg AG1-8X anion exchange resin (chloride form, 100-200 mesh size) was conditioned with 12 M HCl (15 mL). A stock solution was prepared by adding 20 kBq ^{232}U to 12 M HCl (15 mL) which was then passed through the column. Three aliquots of 12 M HCl (10 mL) were passed through the column (fractions I-III). The ^{232}U was eluted with 0.1 M HCl (10 mL, fraction IV). The removal of the daughter isotopes was confirmed by ultra-low background scintillation counting (Quantulus; Perkin Elmer; using α/β discrimination).

The ^{232}U was successfully separated from ^{228}Th (and daughters) with typical ^{232}U recoveries of 80-90% (see Figure 14).
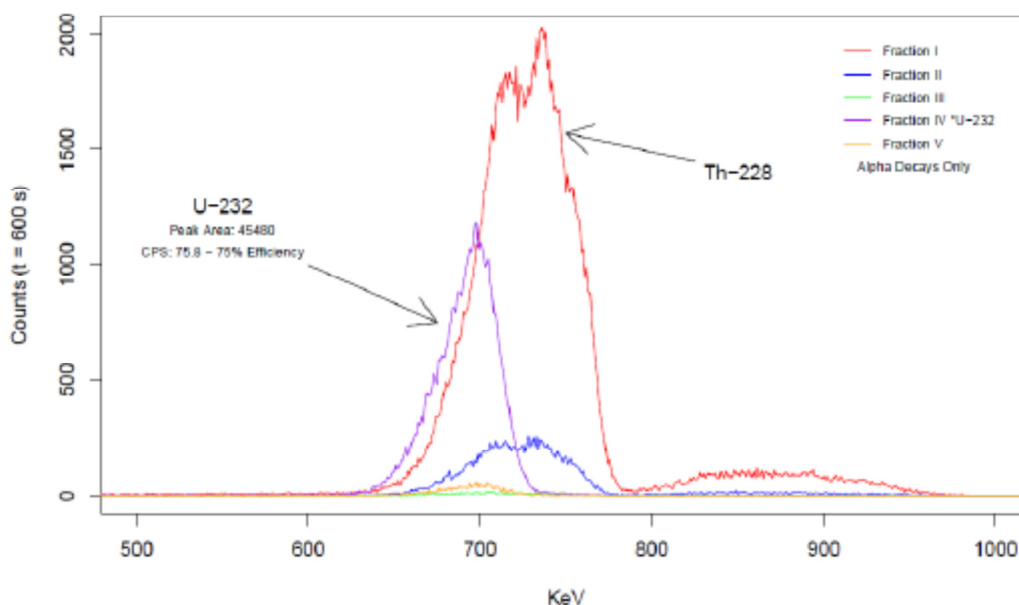

Figure 14: Alpha spectra of ^{232}U separation fractions from a Quantulus ultra low background scintillation counter. ^{232}U (fraction IV) can be seen clearly separated from ^{228}Th (fraction I/II/III).

3.4   Cs and bentonite transport experiments

The authors involved in the work in this section are: T. Missana, M.Garcia-Gutierrez, U.Alonso, N.Albarran and M. Mingarro (*Centro de Investigaciones Energéticas, Medioambientales y Tecnológicas* (*CIEMAT), Madrid, Spain*).

So far, within the BELBaR project, CIEMAT did not carry out specific batch experiments for the analysis of the sorption (ir)reversibility of radionuclides onto bentonite colloids. However, results of transport experiments with cesium and bentonite colloids indicated the reversibility of cesium sorption in the clay particles.

A test of special interest was the one carried out under the Grimsel groundwater conditions (Missana et al 2013). Transport experiments were carried out using water flow velocity from $1 \cdot 10^{-6}$ to $1 \cdot 10^{-5}$ m/s, in an artificial fractures of Grimsel granite from the GTS, injecting cesium ([Cs]=$1 \cdot 10^{-7}$ M) or 100 ppm of bentonite colloids in which Cs was previously adsorbed.

Due to the low salinity of the Grimsel water, more than 80 % of cesium was absorbed onto bentonite particles previous to their injection in the column. The water eluted from the column was analyzed to measure cesium activity and the presence of bentonite colloids by photon correlation spectrometry (PCS) in the same samples and to obtain simultaneously colloid and cesium breakthrough curves.

Figure 15 shows the comparison of the breakthrough curves of cesium in the fracture, obtained without (left) and in the presence (right) of bentonite colloids. The velocity of the water was approximately $3.5 \cdot 10^{-5}$ m/s, with a residence time in the fracture of approximately 2 hours.
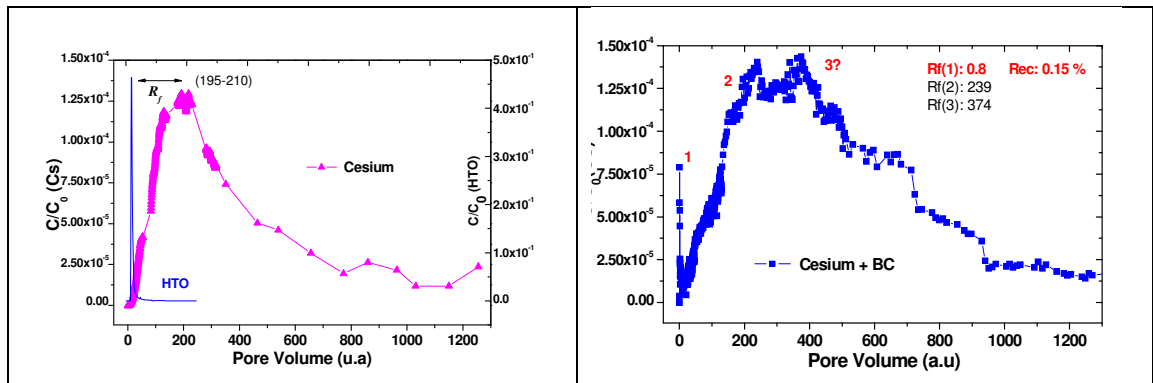

Figure 15: Breakthrough curve of cesium: left, without bentonite colloids; right, in the presence of 100 ppm bentonite colloids

The breakthrough curve of cesium, without colloids, presented a single peak with a retardation factor (Rf) of ~200.

In the presence of bentonite colloids, in the Grimsel case, the breakthrough curve clearly showed a small cesium peak in a position very similar to that of the conservative tracer (HTO), with an Rf of 0.8. Other two peaks were observed in the breakthrough curve with Rf of 200 and 370 approximately. The appearance of new peaks with retardation factors higher than those showed in the same system without colloids, is most probably due to the modification of the sorption properties of the fracture surface caused by bentonite colloid deposition (Albarran et al 2011).

In order to analyze the nature of the first peak observed in the presence of bentonite colloids, in Figure 16, the initial stages of the breakthrough curve of cesium are shown. In the left part, the activity of cesium is plotted and, in the right part, the concentration of colloids measured.

It is quite clear that the first peak of Cs, seen in the breakthrough curve, is coincident with the colloid breakthrough peak measured by PCS. However, the quantity of cesium recovered after this peak was only the 0.15 % of the injected.
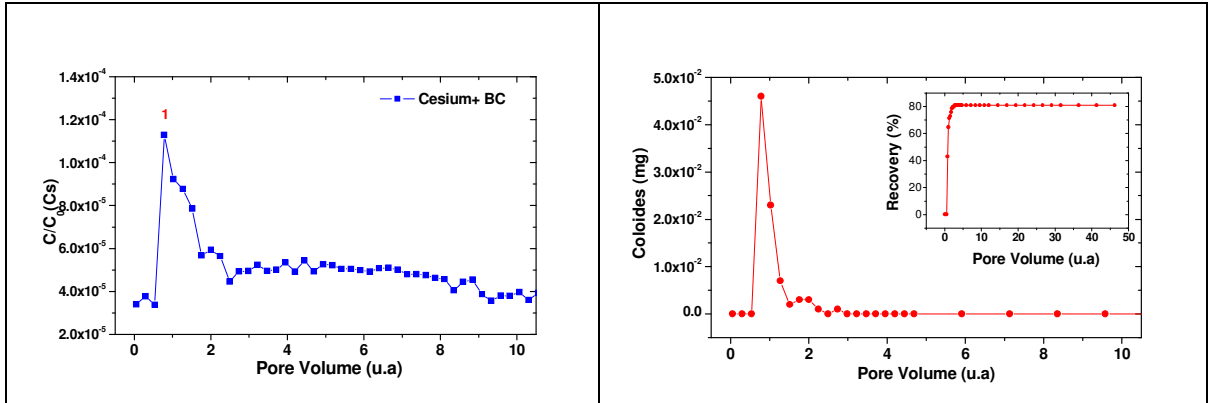

Figure 16: Initial stages of the breakthrough curve of cesium: left, Cs activity measurements; right, PCS measurements (in the inset the recovery of colloids is shown).

The colloid recovery was quite high (80%), and completed after less than 10 pore volumes, therefore if only 0.15% of the injected cesium was recovered at this stage, it means that cesium desorbed from colloid.

It is important to remark that in similar experiments made at CIEMAT with other radionuclides (Sr, Albarran et al 2011; Eu, Missana et al 2008; U Albarran 2010) and bentonite colloids, desorption was also clearly observed. Desorption from the colloids is a very important factor limiting the role of colloids in radionuclide transport.

4 Discussion

4.1 Interactions of $^{237}U/^{237}Pu$ with bentonite/humic systems

In some previous work, the slow sorption over the first few days after contact has been attributed to the formation of humic ternary complexes and slow humic sorption (Pompe et al, 2000). However, given that the U data show no kinetics beyond a few days, it seems unlikely that the steady change in Pu sorption beyond 5 days can be attributed simply to slow humic sorption. For the binary ^{237}Pu/bentonite reaction (before addition of HA), sorption is very rapid, with 70-75% sorption within a few minutes and apparent equilibrium (95% sorbed) within a few hours. The U systems were relatively insensitive to the order of addition, but this is not the case for Pu. Following addition of the humic, there is a reduction in the amount of Pu bound, but in both systems the amount sorbed only falls to approximately 75%, significantly higher than for the system where the humic was added to the Eu prior to the addition of the bentonite. Hence, on the timescale of a few months, and under these particular conditions, there is significant slow dissociation for Pu(III). It is interesting that the 1 and 5 day pre-equilibration systems behave in the same way following the addition of the humic, i.e., in both cases it takes 2-3 days for the amount sorbed to fall to approximately 75%. Given that the amount of Pu sorbed in the 0 day system still appears to be increasing at the end of the experiment, and indeed the other systems may not have reached complete equilibrium (overall, there may be a slight downward trend in the data, particularly for the 1 day system, but given the size of the error bars, this is not certain), it is possible/likely that at some point in the future, the 0 day and 1 and 5 day plots will converge, but this would take a significant amount of time, and certainly a few months at least. Kinetic effects with half-times of this order can have a significant effect upon transport in the real world (see below, will depend upon residence time).

Given that the solid phase and humic are the same for the U and Pu systems, and that both use very low, trace concentrations, it seems likely that it is some difference in the metal ion chemistry that is responsible for the effect, and specifically the nature of the interaction with bentonite.

The behaviour of uranyl in these experiments is consistent with previous studies, which have found only a weak interaction with bentonite colloids and fast kinetics for uranyl (Bouby et al 2010A; Huber et al 2011). The Pu(III) results are also consistent with previous work with trivalent ions (Missana et al 2008; Huber et al 2011), which found stronger association and slow dissociation. This suggests that radionuclide behaviour with bulk bentonite is similar to that with colloidal material.

4.2 Trivalent radionuclide disociation rates

Humic acid is an effective competitor in bentonite systems, and has the advantage of being a ligand that might be present in the vicinity of a repository. However, the work reported here suggests that it introduces considerable complexity and kinetic effects to the system, and so it is probably not a good choice as a competing ligand if the aim is to determine the values of first order rate constants.

Whilst the results from the experiments with EDTA (Figures 10 and 11) are preliminary, they do give us some useful information already. They seem to point towards some kind of relationship between Eu(III)/bentonite pre-equilibration time and the amount that dissociates slowly. The binding of Eu(III) to bentonite in this experiment is showing the same kind of behaviour as reported in the literature. Missana (2008) and Bouby et al (2010, 2011) found that it will associate to the clay, but in the presence of a competitor it will dissociate slowly. Bouby et al (2011) used humic acid as a competitor and reported that on addition of humic acid, an instantaneous, partial initial dissociation of the radionuclide from the bentonite occurred. The same can be seen in these experiments, since on initial addition of EDTA at least 50% of the Eu dissociates immediately. The data are also consistent with the results of Guo et al (2009) who used a pre-

equilibration time of 5 days and then recorded desorption Kd values after a further 5 days. Given that between 50 − 70% of the Eu can be released instantaneously, and the amount remaining bound to the bentonite has fallen to 9 and 14 % for pre-equilibration times of 1 and 7 days, respectively, in these experiments, only a very small difference in K_d value would be expected. This shows the importance of determining dissociation rate constants, rather than just sorption and desorption K_d values, since the K_d values can be very similar, but some part of the dissociation can be very slow. Previous work with organic colloids has shown that in a system where some portion of the radionuclides dissociate slowly, they will dominate transport, even if they account for a very small fraction (<10%) of the total bound radionuclides (Bryan et al 2007). Bouby et al (2010) found that dissociation was slow, taking 1000 hours (42 days), with a maximum pre-equilibration time of 83 days. Depending on the pre-equilibration time, the experiments reported here (for pre-equilibration times less than 115 days), equilibrium is established between 20 and 100 days.

In these experiments, although the systems with longer pre-equilibration times have yet to reach the equilibrium position (dashed line in Figure 10), all of the samples are dissociating towards that limit. Hence, so far no evidence of irreversibility has been observed.

There is a relatively small difference between the rates for the different systems. Superficially, the bentonite dissociation behaviour is similar to that of humic substances, where there is a range of first order dissociation rates from instantaneously dissociating to a distinct long-lived fraction (e.g. King et al 2001), although clearly the mechanisms must be very different. From the data in Table 3 for the experiments conducted so far, the average Eu(III) dissociation rate constant is 1.1×10^{-7} s^{-1}, with an average reaction half time (τ) of 83 days and a range of $1.42 \times 10^{-7} - 5.90 \times 10^{-8}$ s^{-1} ($\tau = 57 - 137$ days).

Bentonite is a mixture (Karnland 2010; Koch 2008), and so it is always possible that the different dissociation rates observed in Figure 11 could be associated with the different components in the mixture, rather than different interactions with the same material. At present, it is not possible to know whether this is the case.

The multiple rate constants observed in the Eu experiments may help to explain the data of Bouby et al (2010C), who found that there appeared to be different apparent dissociation rates in column and batch experiments. If the residence time of the solution in the column experiments is different to the dissociation time in the batch experiments, then it may be that the column experiments access some of the spectrum of rates, whilst the batch experiments access a different selection of dissociation rates.

Wold (2010) estimated dissociation rates for some metal ions: Pu(IV) 4.35×10^{-3} hr^{-1} (= 1.2×10^{-6} s^{-1}); Am(III) 2×10^{-3} hr^{-1} (= 5.6×10^{-7} s^{-1}); Np(IV) 4.6×10^{-7} hr^{-1} (= 1.2×10^{-10} s^{-1}); Cm(III) 6×10^{-3} hr^{-1} (= 1.7×10^{-6} s^{-1}); U(VI) 3×10^{-3} hr^{-1} (= 8.3×10^{-7} s^{-1}); Tc(IV) 0.63 - 15 hr^{-1} (= 1.75×10^{-4} - 4.2×10^{-3} s^{-1}). These values were calculated from Kd values and association rates. We might expect some differences between the values reported here and those of Wold (2010), because Wold's calculation assumes that all of the bentonite bound radionuclide represents a single fraction, whereas, the kinetic data (Figure 11) show at least 3 fractions (instantaneous, faster and slower). Therefore, we would expect Wold's rate constants to be higher than those in Table 3. That said, Wold's rate constant for Am(III) is very close to that recorded here (factor of four higher than average for data in Table 3). The other trivalent rate constant from Wold (2010), for Cm(III), is an order of magnitude higher than the Eu rate. The Cm(III) rate is very similar to that in the 1 day pre-equilibration experiment.

Huber et al (2011) have also provided dissociation rate constants for bentonite colloids from competition experiments using fracture filling material. For Am(III), the values were in the range 1 - 2.5 $\times 10^{-6}$ s^{-1}, whilst for Pu(IV), the range was 3.9×10^{-7} - 2.4×10^{-6} s^{-1}. The rate constants in this study are lower than the Am data from Huber et al (2011). This may be because those are

estimated rates assuming that all of the bound metal dissociates with the same rate, whereas the rate constants in Table 3 are for only a fraction of the colloid bound Eu.

Colloid preliminary experiments

Whilst the colloid characterisation work reported here was largely preliminary, there are still some interesting results to discuss. A colloid concentration could be established using ICP-AES (218 ppm). This, with the information from the SEM-EDX, suggests that bentonite colloids have been created with a size under 500nm. Bouby et al (2011) found that delamination of the stock bentonite LiCl (1 M) increases colloid recovery concentrations. This did not appear to be the case during this investigation. However, the reason could be the initial centrifuge step that ensures the supernatant does not have particles larger than 500 nm. This step is not included in the method of Bouby et al (2011), and it could be that particles have been removed. This will be investigated further.

The ICP-AES analysis performed on the filtered fractions indicates that the majority of bentonite colloids are over 20 nm in size (approximately 98%). Clearly, larger filter sizes should be used in the future.

As ~98% of the colloids are filtered by the first (300 kDa, *ca.* 20 nm) filter, then if the ^{152}Eu(III) is colloid bound it would also not be able to make it through the filter (being stopped with the colloid). Less than 1% of the active sample passed through the largest filter, so most of the radionuclide must have been bound to the bentonite colloids larger than 20 nm.

4.3   Colloid kinetics in the safety case

Although the Eu dissociation experiment is not complete, it does already tell us something about the nature of interaction between the metal ion and the bentonite. The Eu binds to the bentonite quickly, and although there is a subsequent increase in the amount bound by 2.5% and an associated increase in the Kd, it is clear that more than this 2.5% of the Eu changes its interaction with the bentonite, because there is a very different dissociation behaviour for the system with a short pre-equilibration time and those that were equilibrated for more than 1 day. Therefore, it seems that there is rapid uptake to some fraction that is bound, but may be (relatively) easily removed if a stronger sink becomes available. However, over time it seems that there is a transfer of some of the bound Eu to a different fraction that dissociates more slowly. There is also an associated small increase in Kd, which suggests that the transfer may also be associated with an increase in thermodynamic stability. However, some of the material also remains available for instantaneous dissociation, even after several months of contact time. Further, it seems that there are multiple fractions (as shown by the fact that there are multiple first order dissociation rate constants). Figure 17 shows a schematic representation of possible relationships between the different bentonite bound fractions: from the available data it not possible to tell whether access to the different fractions is sequential (Figure 17A) or whether they are unconnected or parallel (Figure 17B).

The test for radionuclide-colloid interactions in the Colloid Ladder (see above) is whether the interaction is 'irreversible'. However, the situation is more complex than such a simple 'yes or no' question. First, no radionuclide sorption and/or incorporation process will truly be irreversible, and given sufficient time any bentonite colloid associated radionuclide will eventually be able to leave the colloid, although that could take a very long time. The important question is whether the time that would be taken for the radionuclide to be released from the colloid is greater or less than the timescale of interest. In the cse of a transport calculation, the important timescale is the residence time, t_{res},

$$t_{res} \; = \; \frac{L}{V}$$

where L is the distance over which the transport takes place and V is the linear velocity of the mobile phase. Calculations that include chemical kinetics are computationally expensive. Most approaches to safety case calculations assume equilibrium, and to include kinetics directly would

be inconvenient. Therefore, it is important to identify exactly when it is necessary to include them explicitly in transport calculations.
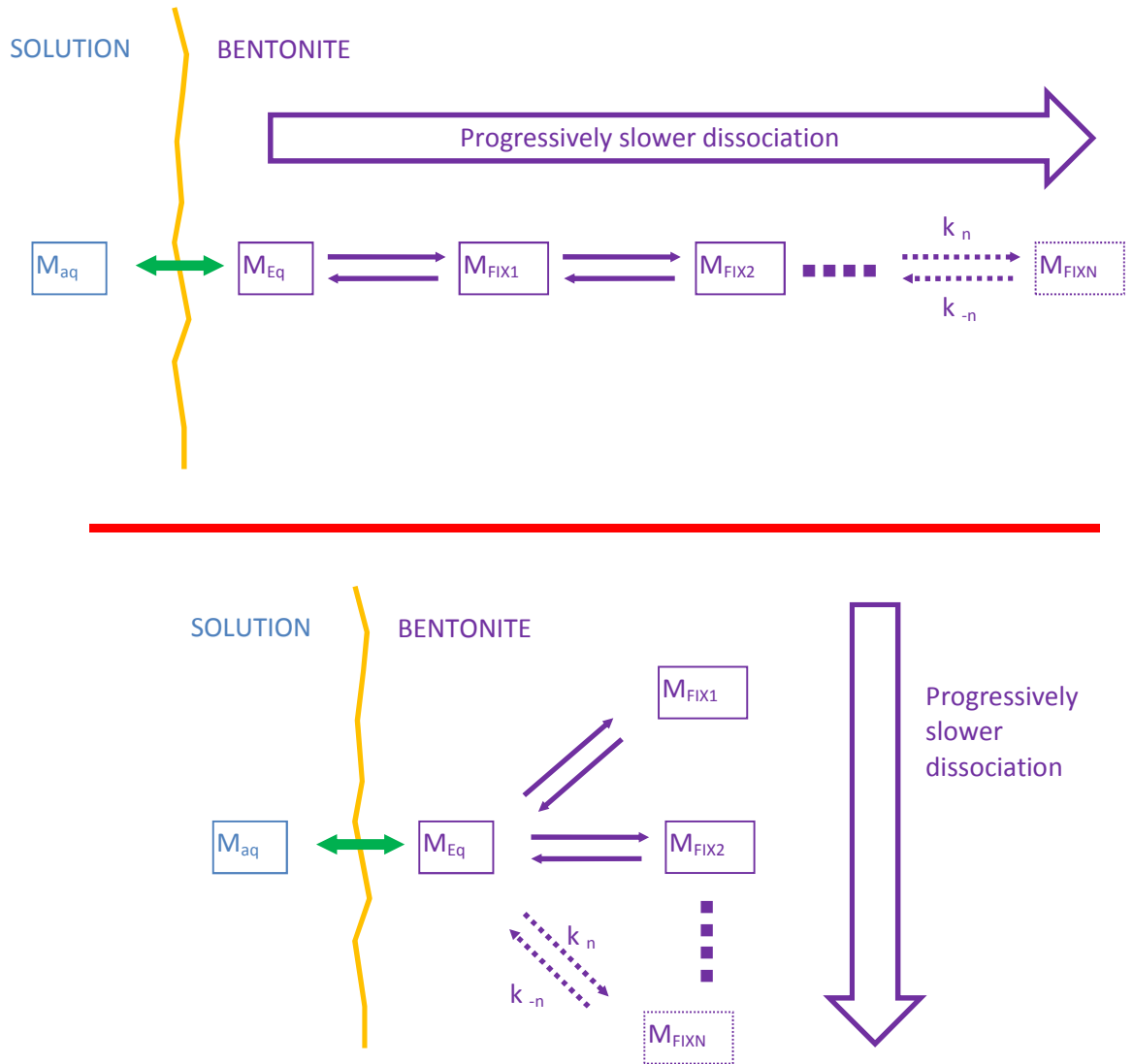

Figure 17A (top), 17B (bottom): schematic representation of the possible interactions of the bentonite bound fractions. M_{aq} = free metal ion; M_{Eq} = instantaneously dissociating; M_{FIX*} = slowly dissociating fractions.

Jennings and Kirkner (1984) found that the behaviour of a species controlled by kinetics may be rationalised using Damkohler numbers. They applied Damkohler numbers to slow sorption onto surfaces during transport. The situation here is different, because the slow reactions involve species in the mobile phase (colloids), rather than the stationary. Bryan et al (2007) used the same type of approach to analyse the effect of slow processes associated with humic substances. The correct value(s) of the dissociation rate constant(s) for bentonite colloids are not yet known, but when they are, we will be able to adapt their method to analyse bentonite kinetics. This section describes a procedure that could be used to assess the importance of slow dissociation kinetics.

The data in Section 3 suggest that more than one dissociation rate constant is required to describe the release of radionuclides from bentonite. However, work with organic colloids has suggested that if a distinct, most long-lived fraction exists, then the effect of slow colloid dissociation on metal ion transport can be predicted from the slowest dissociation rate constant

(Bryan et al 2007, 2012). Preliminary analysis does seem to suggest that there is a distinct fraction for bentonite.

If we consider a simple colloid system with a first order dissociation rate constant that represents a rate determining step for dissociation of radionuclides (Figure 18)
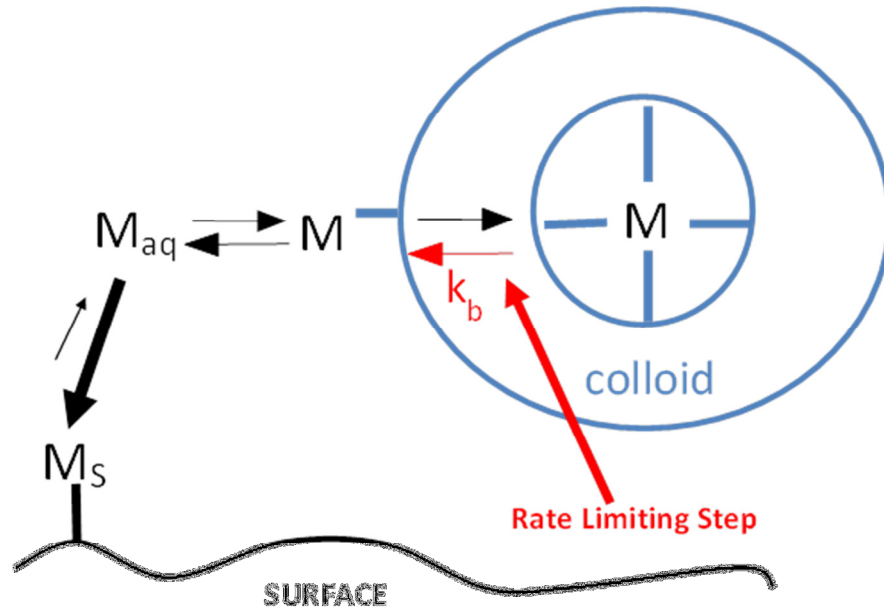

Figure 18: A simplified colloid system with a rate limiting step for dissociation of radionuclides (M) from the colloid to allow immobilisation on the rock surface (M_S) via the free form (M_{aq}).

For such a system, it is possible to calculate the amount of radionuclide that will remain bound to the colloid relatively easily, since it will depend only on the rate constant and the time available for dissociation (which depends on the the distance travelled and the flow rate. Figure 19 shows the dissociation of radionuclides from colloids as a function of residence time: if the time is expressed in units of $1/k_b$, then the plot may be applied to any system. This is the basis of the 'Damkohler approach'.
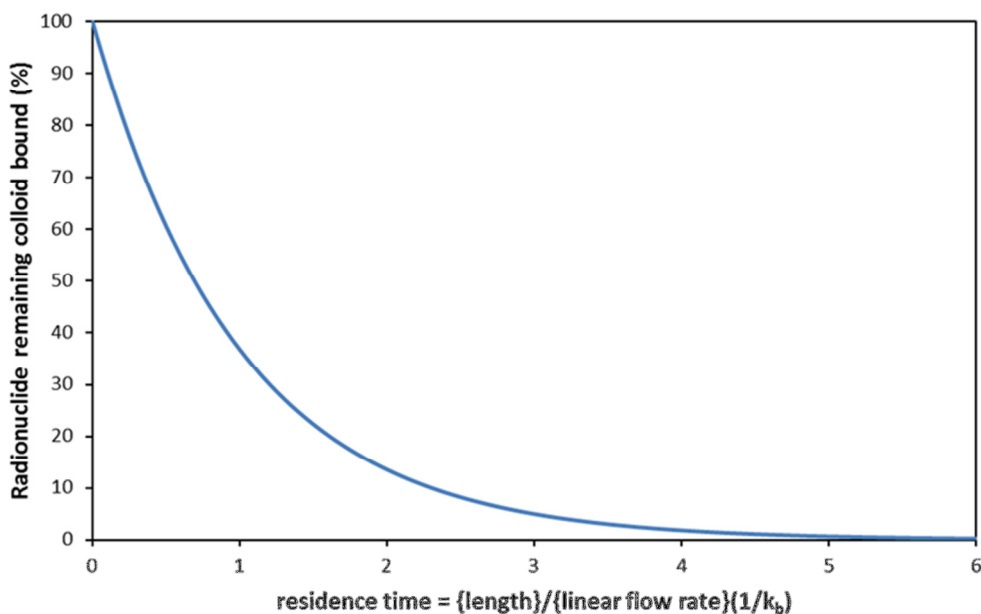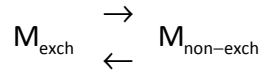

Figure 19: amount of radionuclide remaining colloid bound as a function of residence time, expressed as the reciprocal of the first order dissociation rate constant.

31

In this approach, we consider only two bentonite bound fractions: that available for instantaneous dissociation (exchangeable), M_{exch}; and that affected by the rate limiting slow dissociation (the non-exchangeable), $M_{non-exch}$,

$$M_{exch} \underset{\leftarrow}{\overset{\rightarrow}{}} M_{non-exch}$$

Transfer between the fractions is described with a rate equation,

$$\frac{d[M_{non-exch}]}{dt} = k_f[M_{exch}] - k_b[M_{non-exch}]$$

where k_f and k_b are the first order rate constants for transfer into and out of the slow dissociating fraction, respectively.

The dimensionless Damkohler number for a metal ion (radionuclide) in the slowly dissociating fraction, D_M, is defined by,

$$D_M = \frac{L}{V}k_b$$

where, L is the length of the column, and V is the linear flow rate. The behaviour is controlled by the value of the dissociation rate constant, k_b, and systems with the same values of D_M will show the same behaviour.

As k_b (and so D_M) varies, there are two limiting behaviours. At high values of k_b, dissociation kinetics will be unimportant, and a simple equilibrium (K_d) approach can be used to describe the interaction of the radionuclide with the colloids. At lower k_b, kinetics will dominate the behaviour, and provided that the colloid itself is not retarded, the behaviour of the radionuclide will tend towards that of a conservative tracer.

The distinction between equilibrium and kinetic reactions is always artificial, since it depends upon the time scale of the observation. A reaction that may be treated as an 'equilibrium' over periods of hours, may well be 'slow' on a time scale of seconds. Given the conditions of the transport calculation, flow rate and column length, it is possible to reduce any series of reactions, regardless of origin or chemistry, to just three classes:
1. Those reactions that are sufficiently fast to be treated as equilibria, i.e., high k_b;
2. Those that are sufficiently slow that they effectively do not take place (low k_b);
3. Those reactions that can only accurately be described by the use of rate equations (intermediate k_b).

We may use the limiting behaviours if k_b is sufficiently large or small. Approximations are common in complex systems, but in the case of calculations for a safety case, there is a special requirement that approximations should be conservative. Hence, the viability of approximations will depend upon the application and in the case of R.P.A. whether or not they are conservative.

Approximations
Given that all systems with the same D_M number behave in the same way, we may use D_M to judge the impact of dissociation kinetics, and hence to judge when it is necessary to include kinetics explicitly in transport calculations. As the value of D_M decreases, the non-exchangeably bound metal tends towards the behaviour of a conservative tracer. This gives us our first alternative to including chemical kinetics in the transport calaculations, the 'decoupled' approximation.

Decoupled approximation: For systems with low D_M, virtually no metal ion can leave the non-exchangeable fraction in the time of the calculation. Therefore, the reaction that connects the exchangeable and non-exchangeable may be removed from the calculation and the two fractions are treated as independent species. Beyond the fact that it reduces the mathematical complexity

of the model system (and hence computing time), the advantage of this technique is that it is inherently conservative.

Equilibrium approximation: At the other extreme of high D_M values, the behaviour of the non-exchangeable fraction tends towards that of the exchangeable. Therefore, the alternative approximation, the equilibrium approximation, assumes that the non-exchangeable may be treated with an equilibrium constant or K_d. This will remove the kinetics from the calculation. However, although the behaviour of the non-exchangeable does tend towards that of the exchangeable, it always moves slightly further than the exchangeable, i.e., this approximation may not be conservative. The size of the error will decrease as D_M increases, but it will always be there. The main influence of slow colloid dissociation kinetics is to promote migration. Therefore, any approximation that assumes that kinetics do not exist, would be expected to underestimate transport.

It is possible that the difference between the exact and approximate results might not be significant. For example, for a system with D_M = 30,000, the difference between an exact calculation with a rate constant and one with a K_d is less than 1% (Bryan et al 2007). At intermediate values of D_M, neither the decoupled nor the equilibrium approximations will provide reliable results. To include the kinetic reaction is the only way to produce reliable predictions in this region, although this could be computationally expensive.

Ranges of Validity for Approximations: Ideally, we would like a set of rules that would allow us to decide when to use a given approximation. However, that will depend upon the acceptable error. The equilibrium approximation is particularly problematic, since its estimates are not conservative. The decoupled approach is always conservative, but it could lead to a significant overestimation of transport in many cases.

The point at which the error becomes unaccecptible will depend upon the the application. Once k_b has been properly defined, then it would be possible to define conditions where the two approximations or 'full kinetics' could be used. Figure 20 (linear flow rate vs distance) shows an example: the area is divided into a series of regions. In region A, the decoupled approximation is appropriate, and this will be still be true moving into the slice labelled a, but as we move down and right, the error introduced with the decoupled approximation will get larger and larger, although the prediction will always be conservative. In the bottom right hand corner (region B): the equilibrium approximation will be more appropriate, although as we move up and to the left, towards slice b, the error incurred will become larger, and this time it will not be conservative. In region C, a full treatment of kinetics is best. The arbitrary limits in the figure are based on $k_b = 10^{-7}$ s^{-1} and D_M boundaries of 0.1/0.005 for the decoupled and 100/1000 for equilibrium approximations.
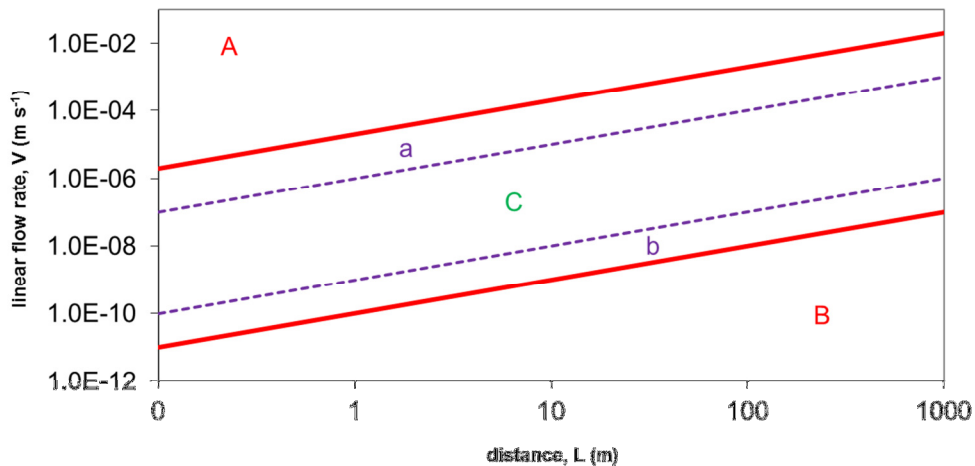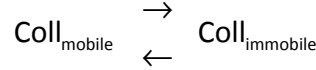

Figure 20: Plot of linear flow rate vs distance showing the regions where the decoupled and equilibrium approximations might be used. Labels explained in the text.

Calculations including the sorption/stability of colloids

The Damkohler treatment thus far has taken no account of the sorption of colloids during transport or colloid instability (aggregation processes, etc.). Colloid sorption and stability are complex processes and they are not the subject of this report. However, both can be slow. For the purposes of the following analysis, we will combine all processes that could remove colloids (and hence radionuclides associated with them) into a single combined reaction linking colloids in solution, $Coll_{mobile}$, with those removed from solution by any process, $Coll_{immobile}$,

$$Coll_{mobile} \quad \overset{\rightarrow}{\underset{\leftarrow}{}} \quad Coll_{immobile}$$

Transfer between the fractions is described with a rate equation,

$$\frac{d[Coll_{immobile}]}{dt} = k_a[Coll_{mobile}] - k_d[Coll_{immobile}]$$

where k_a and k_d are the first order rate constants for transfer out of and back into solution, respectively. Provided that the radionuclide concentration is low, then they should not affect the behaviour of the colloid itself, and so any colloid bound radionuclides will be affected by the same rate constants.

In the case of the interaction of the radionuclides with the colloids, it is only the dissociation rate constant, k_b, that makes a significant difference. Here, both the forward, k_a, and backward rate constants, k_d, make a difference.

Radionuclide behaviour in a system with both colloid sorption/instability and slow dissociation is harder to rationalise than systems where colloids transport conservatively, or with independent kinetic processes, because here they interact. The rate of the colloid removal process affects the residence time of the colloid in the groundwater, and hence the relative effect of the radionuclide dissociation rate.

We can define a Damkohler number for the colloid removal process, D_C,

$$D_C = \frac{k_a}{V}L$$

As D_C approaches zero, the behaviour of the colloid (and any associated radionucliode) will tend towards that of a conservative tracer, whilst as D_C tends to infinity, the extent of sorption will increase, and tend towards equilibrium behaviour, in which case the amount of colloid removed from solution at any point and time is given by,

$$[Coll_{immobile}] = K_C[Coll_{mobile}]$$

where,

$$K_C = \frac{k_a}{k_d}$$

At the upper and lower limits, a kinetic calculation may be avoided by assuming that the colloid complex either: does not sorb at all, and so transports with the velocity of the groundwater (low D_C); or that it does sorb, and that the interaction may be described with an equilibrium constant, K_C (high D_C). Assuming that the colloid does not sorb will give a conservative prediction, whilst the equilibrium approach will not, since the equilibrium assumption produces the maximum possible retardation, and the real behaviour only tends to this as D_C increases. At intermediate values only a full kinetic description will provide a reliable prediction.

If a colloid with an associated radionuclide is removed from solution, then that in itself will cause some retardation. However, it will also increase the residence time of the complex in the water column, allowing more time for dissociation of the radionuclide and immobilisation on the rock surface. The extent of this effect will depend upon the affinity of the complex for the surface and the colloid Damkohler number (D_C). If D_C is small, then the residence time is too short for removal

from solution to be significant, the complex transports with the velocity of the groundwater, and there is no effect upon the metal-humic kinetics, i.e. the behaviour of the metal is still controlled solely by k_b, and D_M may still be used to define the behaviour of the contaminant,

$$D_M = \left.\frac{k_b}{V}L\right|_{D_C \to 0}$$

However, in the case of significant retardation of the colloid, the Damkohler number for the slowly dissociating radionuclide must be adapted to take account of the increased residence time. If D_C is large ($D_C \to \infty$), and the humic sorption process may be described with an equilibrium constant, K_C, then the effective metal ion Damkohler number, D_M^{eff}, will be given by,

$$D_M^{eff} = \left.\frac{k_b}{V}L\,(1+K_C)\right|_{D_C \to \infty}$$

For systems with intermediate values of D_C, these equations may be used to provide a range of Damkohler numbers, the most representative value lying somewhere in between.

To assess the importance of slow dissociation kinetics in a system that includes colloid immobilisation processes and to determine the most appropriate approximations, first one should calculate D_C. If it is small, then D_M may be used to determine whether slow dissociation kinetics are significant, whilst if it is large, D_M^{eff} should be used. If D_C has an intermediate value, then D_M will provide an indication of the maximum possible effect of slow dissociation, and D_M^{eff} the minimum. Figure 21 shows the procedure that should be used for selecting the most appropriate approximations if any, to describe slow dissociation and colloid removal processes. The flow sheet in the figure provides the most appropriate approximations (if any) for systems including colloid immobilisation and slowly dissociating radionuclides. MAX1 and MIN1 are the arbitrary Damkohler number limits for the colloid removal, and MAX2 and MIN2 are the limits for the slow dissociation of radionuclides from colloids. These values would depend upon the requirements of the calculation and the acceptable errors.

Depending upon D_C and D_M or D_M^{eff}, there are 9 possible options, 5 of which are conservative and 4 non-conservative. 4 of the options avoid all kinetic equations, another 4 include 1 kinetic process, and only one option requires a kinetic description of both colloid removal and slow dissociation. Of course, the exact solution with a kinetic description of both processes will always give the correct solution, but that will require the longest calculation times.
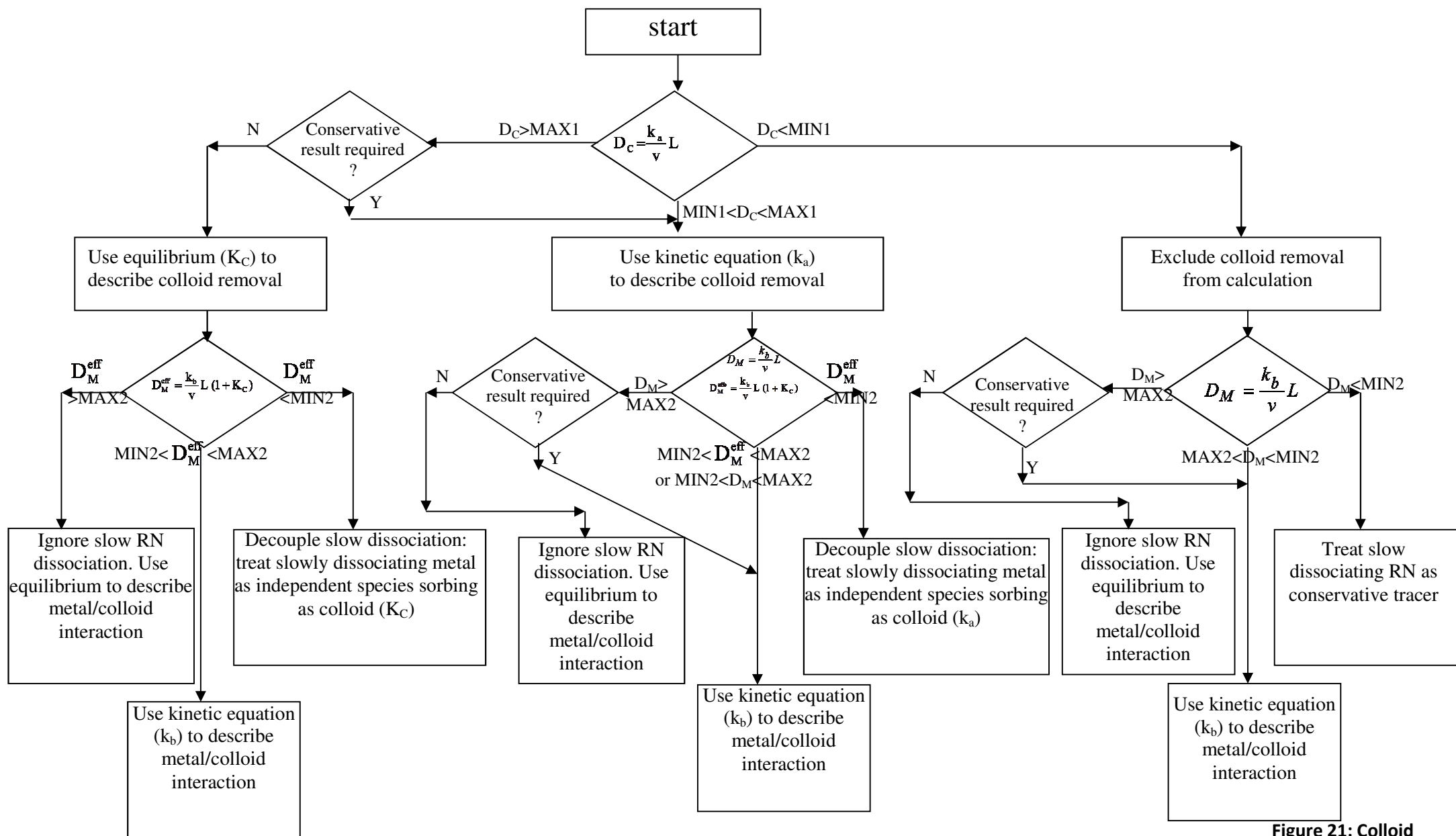
35

start

Conservative result required ?

$D_C = \frac{k_a}{v} L$

$D_C > MAX1$ $D_C < MIN1$ $MIN1 < D_C < MAX1$

N   Y

Use equilibrium (K_C) to describe colloid removal

Use kinetic equation (k_a) to describe colloid removal

Exclude colloid removal from calculation

D_M^{eff} >MAX2 $D_M^{eff} = \frac{k_b}{v} L (1 + K_C)$ D_M^{eff} <MIN2

MIN2< D_M^{eff} <MAX2

Ignore slow RN dissociation. Use equilibrium to describe metal/colloid interaction

Decouple slow dissociation: treat slowly dissociating metal as independent species sorbing as colloid (K_C)

Use kinetic equation (k_b) to describe metal/colloid interaction

Conservative result required ?   N $D_M >$ MAX2

$D_M = \frac{k_b}{v} L$

$D_M^{eff} = \frac{k_b}{v} L (1 + K_C)$

D_M^{eff} <MIN2

MIN2< D_M^{eff} <MAX2 or MIN2<D_M<MAX2

Y

Ignore slow RN dissociation. Use equilibrium to describe metal/colloid interaction

Decouple slow dissociation: treat slowly dissociating metal as independent species sorbing as colloid (k_a)

Use kinetic equation (k_b) to describe metal/colloid interaction

Conservative result required ?   N $D_M >$ MAX2

$D_M = \frac{k_b}{v} L$

$D_M < MIN2$

MAX2<D_M<MIN2

Y

Ignore slow RN dissociation. Use equilibrium to describe metal/colloid interaction

Treat slow dissociating RN as conservative tracer

Use kinetic equation (k_b) to describe metal/colloid interaction

Figure 21: Colloid kinetics flowsheet.

5   Conclusions

The bentonite dissociation experiments show that the binding of Eu(III) and Pu(III) to bentonite shows no sign of being irreversible at the moment. Like other trivalent systems studied previously, it does sorb to the clay but will dissociate over time in presence of a competing ligand.

It seems that uranyl does not show slow dissociation kinetics. The results here that show relatively rapid reversibility are consistent with previous work with bentonite colloids. It seem that colloidal and bulk bentonite have very similar interactions with radionuclides (which is hardly surprising).

Interestingly, the results could suggest that there is an increase in the amount of radionuclide that dissociates slowly as pre-equilibration time increases. The experiments suggest that there is a change in dissociation behaviour between pre-equilibration times of 1 day and 1 week, with a reduction in the slowest dissociation rate constant of approximately an order of magnitude. For pre-equilibration times of more than 1 week, there is evidence for multiple dissociation rates, in addition to a significant fraction that dissociates instantaneously. There does seem to be a distinct most slowly dissociating fraction that has a characteristic rate constant of approximately 10^{-7} s^{-1}. The amount of this fraction definitely increases over the first week of pre-equilibration from 0 to 17 %. Thereafter, the amount seems to increase further, reaching approximately 27 % by 115 days. However, these data are preliminary, and experiments continue.

Significantly, there is no evidence for irreversible binding of Eu(III) and Pu(III), because it is possible that all of the systems described here might return to equilibrium given sufficient time. However, dissociation is slow, and the first order dissociation constant is such that it could affect radionuclide transport, depending upon the distance and flow rate of the system.

One might think that, because of the long calculation times involved in safety case calculations, which can be of the order of hundreds of thousands of years, that chemical kinetics cannot be important. However, it is not the total simulation time that matters, but the residence time in the groundwater, which is likely be considerably shorter. Hence, slow dissociation from colloids could be important, even for long-term calculations.

The most appropriate slow dissociation rate constants are not yet certain, and they will depend upon the radionuclide. When we do have the rate constants, we have a set of rules based on Damkohler numbers that will allow us to determine the importance of kinetics, and to determine the validity of approximations.

Whilst the colloid work is of a preliminary nature, it will be useful for the future direct determination of colloid dissociation rates. It has been shown that bentonite colloids can be generated and characterised. The stock solutions will be suitable for kinetic experiments in the next stage of the project.

The ultrafiltration coupled with ICP-AES analysis and gamma ray spectrometry shows that ^{152}Eu(III) binds to the bentonite colloids, and that this colloidal suspension has particles that are larger than 20 nm.

Next Steps

The colloid work is ready to move onto the next stage. More thorough filtration of the colloid stock will give a greater understanding of the colloid size distribution. Several fractions over the entire colloid size range (1–500 nm) will be collected, and their concentrations will be analysed via a combination of ICP-AES and SEM-EDX. Eu(III) will be added to colloid solutions prior to ultrafiltration to determine its size distribution too. Competing solid phases will be tested to explore the dissociation kinetics of the radionuclides bound to the colloids.

The Eu(III) batch experiments are continuing, and analysis will continue in the future to give more dissociation kinetic data.

^{232}U and ^{228}Th preliminary experiments are in progress. Batch bulk type experiments will be performed in much the same way as the ^{152}Eu experiments. Once the colloid dissociation rate techniques have been finalised using Eu, the experiments will be extended to ^{232}U and ^{228}Th.

Acknowledgements

References

N. Albarran, 2010, Ph.DThesis, Procesos de migración de contaminantes asociados a coloides en un almacenamiento geológico de residuos radiactivos, Universidad Autónoma de Madrid (In Spanish).

N. Albarran, T. Missana, M. Garcia-Gutierrez, U. Alonso, M. Mingarro, 2011. Journal of Contaminant Hydrology, 122, 2011, 76-85.

M. Bouby, A. Filby, H. Geckeis, F. Geyer, R. Götz, W. Hauser, F. Huber, S. Keesmann, B. Kienzler, P. Kunze, M. Küntzel, J. Lützenkirchen, U. Noseck, P. Panak, M. Plaschke, A. Pudewills, T. Schäfer, H. Seher, C. Walther, 2010A, Sorption reversibility studies: Comparison of fracture filling material (FFM) from Grimsel (Switzerland) and Äspö (Sweden) in *Colloid/Nanoparticle formation and mobility in the context of deep geological nuclear waste disposal (Project KOLLORADO-1; Final report),* Thorsten Schäfer & Ulrich Noseck (Eds.), FZKA Wissenschaftliche Berichte, FZKA 7515, pg 25 - 36.

M. Bouby, A. Filby, H. Geckeis, F. Geyer, R. Götz, W. Hauser, F. Huber, S. Keesmann, B. Kienzler, P. Kunze, M. Küntzel, J. Lützenkirchen, U. Noseck, P. Panak, M. Plaschke, A. Pudewills, T. Schäfer, H. Seher, C. Walther, 2010B, Core migration studies in *Colloid/Nanoparticle formation and mobility in the context of deep geological nuclear waste disposal (Project KOLLORADO-1; Final report),* Thorsten Schäfer & Ulrich Noseck (Eds.), FZKA Wissenschaftliche Berichte, FZKA 7515, pg 25 - 36.

M. Bouby, A. Filby, H. Geckeis, F. Geyer, R. Götz, W. Hauser, F. Huber, S. Keesmann, B. Kienzler, P. Kunze, M. Küntzel, J. Lützenkirchen, U. Noseck, P. Panak, M. Plaschke, A. Pudewills, T. Schäfer, H. Seher, C. Walther, 2010C, *Colloid/Nanoparticle formation and mobility in the context of deep geological nuclear waste disposal (Project KOLLORADO-1; Final report),* Thorsten Schäfer & Ulrich Noseck (Eds.), FZKA Wissenschaftliche Berichte, FZKA 751.

M. Bouby, H. Geckeis, J. Lutzenkirchen, S. Mihai, T. Schafer, 2011, Interaction of bentonite colloids with Cs, Eu, Th and U in presence of humic acid: A flow field-flow fractionation study, Geochimica et Cosmochimica Acta, 75, 3866–3880.

M.H. Bradbury, B. Baeyens, H. Geckeis, T. Rabung, 2005, Sorption of Eu(III)/Cm(III) on Ca-montmorillonite and Na-illite. Part 2: Surface complexation modelling, Geochimica et Cosmochimica Acta, 69, 5403–5412.

M.H. Bradbury B. Baeyens, 1999, Modelling the sorption of Zn and Ni on Ca-montmorillonite, Geochimica et Cosmochimica Acta, 63, 325–336.

M.H. Bradbury B. Baeyens, 2006, Modelling sorption data for the actinides Am(III), Np(V) and Pa(V) on montmorillonite Radiochim. Acta, 94, 619–625.

N.D. Bryan, D.L.M. Jones, R.E. Keepax, D.H. Farrelly, L.G. Abrahamsen, P. Warwick, N. Evans, 2007, The Role of Humic Non-Exchangeable Binding in the Promotion of Metal Ion Transport in the Environment, Journal of Environmental Monitoring, 9, 329-347.

N.D. Bryan, L. Abrahamsen, N. Evans, P. Warwick, G. Buckau, L.P. Weng and W.H. Van Riemsdijk, 2012, The effects of humic substances on the transport of radionuclides: Recent improvements in the prediction of behaviour and the understanding of mechanisms. Applied Geochemistry, 27, 378-389.

R.N.J. Comans, 1987, Adsorption, desorption and isotopic exchange of cadmium on illite: evidence for complete reversibility. Water Research, 21, 1573–1576.
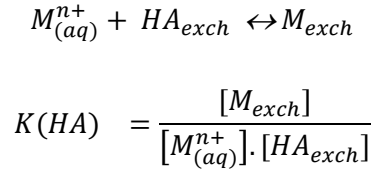
R.N.J. Comans, M. Haller, P. Depreter, 1991, Sorption of cesium on illite – nonequilibrium behavior and reversibility. Geochimica Cosmochimica Acta, 55, 433–440.

A. de Koning, R.N.J. Comans, 2004, Reversibility of radiocaesium sorption on illite. Geochimica Cosmochimica Acta, 68, 2815–2823.

A. Delos, C.Walther, T. Schaefer and S. Buechner, 2008, Size dispersion and colloid mediated radionuclide transport in a synthetic porous media. Journal of Colloid and Interface Science, 324, 212-215.

H. Geckeis, T. Schäfer, W. Hauser, T. Rabung, T. Missana, C. Degueldre, A. Möri, J. Eikenberg, T. Fierz, W.R. Alexander, 2004, Results of the Colloid and Radionuclide Retention experiment (CRR) at the Grimsel Test Site (GTS), Switzerland -Impact of reaction kinetics and speciation on radionuclide migration. Radiochimica Acta. 92, 765-774.

Z. Guo, J. Xu, K. Shi, Y. Tang, W. Wu, Z. Tao, 2009, Eu(III) adsorption/desorption on Na-bentonite: Experimental and modeling studies. Colloids and Surfaces A: Physicochemical and Engineering Aspects, 339, 126–133.

W. Hauser, H. Geckeis, J.I. Kim, T. Fierz, 2002, A mobile laser-induced breakdown detection system and its application for the in situ-monitoring of colloid migration. Colloids and Surfaces A: Physicochemical and Engineering Aspects, 203, 37-45.

B.D. Honeyman, 1999, Colloidal culprits in contamination. Nature, 397, 23–24.

F. Huber, P. Kunze, H. Geckeis, T. Schäfer, 2011, Sorption reversibility kinetics in the ternary system radionuclide-bentonite colloids/nanoparticles-granite fracture filling material. Applied Geochemistry, 26, 2226–2237.

K. Iijima, T. Tomura, M. Tobita and Y. Suzuki, 2010, Distribution of Cs and Am in the solution-bentonite colloids-granite ternary system: effect of addition order and sorption reversibility. Radiochimica Acta, 98, 729–736.

P. Ivanov, T. Griffiths, N.D. Bryan, G. Bozhikov and S. Dmitriev, 2012, The effect of humic acid on uranyl sorption onto bentonite at trace uranium levels. J. Environ. Monit., 14, 2968–2975.

A.A. Jennings and D.J. Kirkner, 1984, Instantaneous equilibrium approximation analysis. Journal of Hydraulic Engineering (A.S.C.E.), 110, 1700 – 1717.

O.Karnland, 2010, Chemical and mineralogical characterization of the   bentonite buffer for the acceptance control procedure in a KBS-3 repository, SKB Technical Report, TR-10-60.

A. Kersting, D. Efurd, D. Finnegan, D. Rokop, J. Thompson, 1999, Migration of plutonium in the groundwater at the Nevada Test Site, Nature, 397, 56–59.

S.J. King, P. Warwick, A. Hall, N.D. Bryan, 2001, The dissociation kinetics of dissolved metal-humic complexes. Physical Chemistry Chemical Physics, 3, 2080-2085.

D. Koch, 2008, European bentonites as an alternative to MX-80, Science & Technology series no 334.

A. Kowal - Fouchard, R. Drot, E. Simoni , J. Ehrhardt, 2004, Use of Spectroscopic Techniques for Uranium(VI)/ Montmorillonite Interaction Modeling. Environmental Science and Technology, 38, 1399-1407.

P. Kunze, H. Seher, W. Hauser, P.J. Panak, H. Geckeis, Th. Fanghänel, T. Schäfer, 2008, The influence of colloid formation in a granite groundwater bentonite porewater mixing zone on radionuclide speciation. Journal of Contaminant Hydrology, 102, 263–272.

M. Laaksoharju, S. Wold, 2005, The colloid investigations conducted at the Aspo Hard Rock Laboratory during 2000 – 2004, SKB Technical Report, TR-05-20.

W. Miller, R. Alexander, N. Chapman, I. McKinley, J. Smellie, 1994, Natural analogue studies in the geological disposal of radioactive waste. Studies in Environmental Science, 57.

D. Mihoubi, A.Bellagi, 2006, Thermodynamic analysis of sorption isotherms of bentonite. J. Chem. Thermodynamics, **38**, 1105.

T. Missana, Ú. Alonso, M. García-Gutiérrez, and M. Mingarro, 2008, Role of bentonite colloids on europium and plutonium migration in a granite fracture. Applied Geochemistry, 23, 1484-1497.

T. Missana, Ú. Alonso, M.J. Turrero, 2003, Generation and stability of bentonite colloids at the bentonite/granite interface of a deep geological radioactive waste repository. Journal of Contaminant Hydrology, 61, 17-31.

T. Missana, M.Garcia-Gutierrez, U.Alonso, N.Albarran, M. Mingarro.Cesium migration in granite fractures in the presence of bentonite colloids: comparison between the Grimsel and the Äspö case. Abstract Accepted at the 2013 Migration Conference.

J. Monsallier, W. Schuessler, G. Buckau, T. Rabung, J. Kim, D. Jones, R. Keepax, N. Bryan, 2003, Kinetic Investigation of Eu(III)-Humate Interactions by Ion Exchange Resins. Analytical Chemistry, 75, 13, 3168-3174.

A. Möri, W.R. Alexander, H. Geckeis, W. Hauser, T. Schäfer, J. Eikenberg, T. Fierz, C. Degueldre, T. Missana, 2003, The colloid and radionuclide retardation experiment at the Grimsel Test Site: influence of bentonite colloids on radionuclide migration in a fractured rock. Colloids and Surfaces A: Physicochemical and Engineering Aspects, 217, 33-47.

J.D. Morton, J.D. Semrau, K.F. Hayes, 2001, An X-ray absorption spectroscopy study of the structure and reversibility of copper adsorbed to montmorillonite clay. Geochimica et Cosmochimica Acta, 65, 2709–2722.

Nagra 1994, Technical Report, NTB 94-06.

M. Ochs, B. Lothenbach, M. Shibata, H. Sato, M. Yui, 2003, Sensitivity analysis of radionuclide migration in compacted bentonite: a mechanistic model approach. Journal of Contaminant Hydrology, 61, 313– 328.

A. Pitois, P. I. Ivanov, L. G. Abrahamsen, N. D. Bryan, R. J. Taylor, H. E. Sims, 2008, Magnesium hydroxide bulk and colloid-associated 152Eu in an alkaline environment: Colloid characterization and sorption properties in the presence and absence of carbonate. Journal of Environmental Monitoring, 10, 315-24.
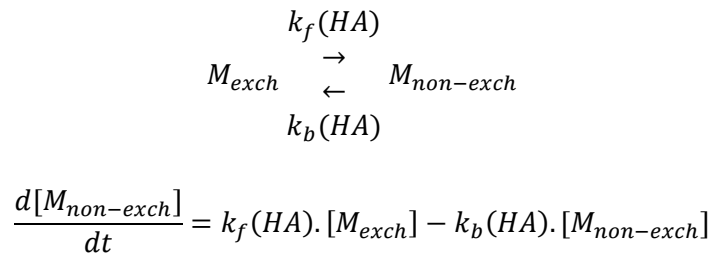
S. Pompe, K. Schmeide, M. Bubner, G. Geipel, K.H. Heise, G. Bernhard and H.Nitsche, 2000, Investigation of humic acid complexation behavior with uranyl ions using modified synthetic and natural humic acids. Radiochim. Acta, **88**, 553.

Th. Rabung, M.C. Pierret, A. Bauer, H. Geckeis, M.H. Bradbury and B. Baeyens, 2005, Sorption of Eu(III)/Cm(III) on Ca-montmorillonite and Na-illite. Part 1: Batch sorption and time-resolved laser fluorescence spectroscopy experiments. Geochimica et Cosmochimica Acta, 69, 5393–5402.

J.N. Ryan, M. Elimelech, 1996, Review: colloid mobilization and transport in groundwater. Colloid Surface A, 107, 1–56.

T. Schäfer, H. Geckeis, M. Bouby, T. Fanghänel, 2004, U, Th, Eu and colloid mobility in a granite fracture under near-natural flow conditions. Radiochimica Acta. 92, 731-737.

T. Schäfer, F. Huber, H. Seher, T. Missana, U. Alonso, M. Kumke, S. Eidner, F. Claret, F. Enzmann, 2012, Nanoparticles and their influence on radionuclide mobility in deep geological formations. Applied Geochemistry, 27, 390–403.

N. Stankovic, M. Logar, J. Lukovic, J. Pantic, M. Miljevic, B. Babic, A. Radosavljevic-Mihajlovic, 2011, Characterization of bentonite clay from "Greda" deposit. Processing and application of ceramics, 5, 97-101.

T. Stumpf, C. Hennig, A. Bauer, M. A. Denecke, T. Fanghänel, 2004, An EXAFS and TRLFS study of the sorption of trivalent actinides onto smectite and kaolinite. Radiochimica Acta 92, 133–138.

S. Wold, 2010, Sorption of prioritized elements on montmorillonite colloids and their potential to transport radionuclides, SKB Technical Report, TR-10-20.

Sh.M. Yu, A.P. Ren, Ch.L. Chen, Y.X. Chen and X. Wang, 2006, Effect of pH, ionic strength and fulvic acid on the sorption and desorption of cobalt to bentonite. Appl. Rad. Isot., **64**, 455.

APPENDIX A: Model Details for Section 3.2

Previous work has shown that the initial interaction between europium ions and humics is a rapid uptake of aqueous $Eu^{3+}_{(aq)}$ by humic acid to an 'exchangeable fraction', which is expected to be an instantaneous reversible process and expressed generally as (Bryan et al 2007, 2012):
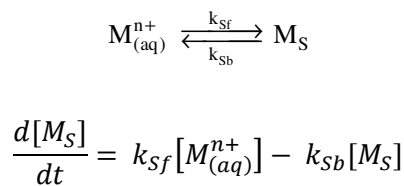
$$M^{n+}_{(aq)} + HA_{exch} \leftrightarrow M_{exch}$$

$$K(HA) = \frac{[M_{exch}]}{[M^{n+}_{(aq)}].[HA_{exch}]}$$

where, HA_{exch} is the HA exchangeable binding site, M_{exch} is the metal ion bound to HA in the exchangeable fraction and K(HA) is the equilibrium constant for the process. The second successive component is a first-order slow transfer of the exchangeable metal (M_{exch}) to a 'non-exchangeable' fraction, $M_{non-exch}$,

$$M_{exch} \quad \overset{k_f(HA)}{\underset{k_b(HA)}{\underset{\leftarrow}{\rightarrow}}} \quad M_{non-exch}$$

$$\frac{d[M_{non-exch}]}{dt} = k_f(HA).[M_{exch}] - k_b(HA).[M_{non-exch}]$$

where, $k_f(HA)$ and $k_b(HA)$ are the forward and backward rate constants, respectively.

In all the modelling data here, the total europium concentration in the system is 7.9×10^{-10} mol L^{-1}. The data do not define the total concentration of humic exchangeable binding sites ($[HA_{exch}]$). Only the product of the equilibrium constant and the binding site concentration (K_{exch} x $[HA_{exch}]$) has been defined. Therefore, an arbitrary value of 1 was selected for the humic binding site concentration in a solution of [HA] = 100 ppm. The values were reduced in proportion to the concentration of the humic sample, i.e., 0.5, 0.25 and 0.1 for 50, 20 and 10 ppm humic acid systems, respectively. Note, because of the assumptions inherent in the model, it can only be applied to systems where the metal ion concentration is insignificant compared to the concentration of humic binding sites.

The interaction of the metal ion with the surface is described with a kinetic K_d approach,

$$M^{n+}_{(aq)} \underset{k_{Sb}}{\overset{k_{Sf}}{\rightleftharpoons}} M_S$$

$$\frac{d[M_S]}{dt} = k_{Sf}[M^{n+}_{(aq)}] - k_{Sb}[M_S]$$

where, k_{Sf} and k_{Sb} are the forward and backward rate constants, respectively and M_S is the metal complexed directly to the surface. Surface complexation models treat the surface as composed of functional groups able to form complexes with metal ions adsorbed from solution. Very often, either one or two metal complexation reactions and stability constants are defined, and typically, they include routines to account for the electrostatic interaction between metal ions and the surface (Dzombak and Morel 1990). Therefore, the approach developed here is simpler than a surface complexation model, The kinetic Kd approach applied here is limited again to trace level experiments.

Three simple mathematical models were developed to simulate the behaviour of the europium ions and humic acid in the experiments. The management of the binary interactions between the humic acid and metal ion and that between the metal ion and the mineral surface are common to all three models, which have been named Models 1, 2 and 3. The chemical and model equations are shown for Model 3 in Table A1. For the interaction of the metal ions direct with the solution phase humic, all three models use the same equations. There is initial, fast uptake to an exchangeable fraction followed by a slower transfer to a single non-exchangeable fraction. A single kinetic equation simulates the interaction of the metal ion with the surface.

Table A1: Equations for model 3: HA_{exch} – humic exchangeable binding site, Eu_{exch} and $Eu_{non-exch}$ –humic bound exchangeable and non-exchangeable Eu, S_M – surface metal binding sites, Eu_S - Eu sorbed to the surface. Units: K(HA1); K(HA2) $dm^3 mol^{-1}$; k_{sb}, k_{HAb}, k_{HAf}, $kb(HA_1+S_1)$, $kb(HA_1+S_2)$, $kb(HA_2+S_1)$, $kb(HA_2+S_2)$ s^{-1}; $ksf=dm^3 mol^{-1} s^{-1}$; $kf(HA_1+S_1)$, $kf(HA_1+S_2)$, $kf(HA_2+S_1)$, $kf(HA_2+S_2)$ $ppm^{-1} s^{-1}$.

No	General Calculations	
1	$Eu^{3+}_{(aq)} + HA_{1exch} \leftrightarrow Eu_{exch,1}$, $K(HA1) = \frac{[Eu_{exch,1}]}{[Eu^{3+}_{(aq)}][HA_{1exch}]}$	$Eu^{3+}_{(aq)} + HA_{2exch} \leftrightarrow Eu_{exch,2}$, $K(HA2) = \frac{[Eu_{exch,2}]}{[Eu^{3+}_{(aq)}][HA_{2exch}]}$
2	$Eu_{exch} \leftrightarrows Eu_{non-exch}$, $\frac{d[Eu_{non-exch}]}{dt} = kfHA[Eu_{exch}] - kbHA[Eu_{non-exch}]$	
3	$Eu^{3+}_{(aq)} + S_M \leftrightarrows Eu_S$, $\frac{d[Eu_{S_1}]}{dt} = ksf[Eu^{3+}_{(aq)}][S_M] - ksb[Eu_S]$	
	Model 3 – humic surface site 1	
4A	$HA_{1free} + S_1 \leftrightarrows HA_1S_1$	$\frac{d[HA_1S_1]}{dt} = kf(HA_1 + S_1)[HA_{1free}][S_1] - Kb(HA_1 + S_1)[HA_1S_1]$
5A	$HA_{2free} + S_1 \leftrightarrows HA_1S_1$	$\frac{d[HA_2S_1]}{dt} = kf(HA_2 + S_1)[HA_{2free}][S_1] - kb(HA_2 + S_1)[HA_2S_1]$
	Model 3 – humic surface site 2	
4B	$HA_{1free} + S_2 \leftrightarrows HA_1S_2$	$\frac{d[HA_1S_2]}{dt} = kf(HA_1 + S_2)[HA_{1free}][S_2] - kb(HA_1 + S_2)[HA_1S_2]$
5B	$HA_{2free} + S_2 \leftrightarrows HA_2S_2$	$\frac{d[HA_2S_2]}{dt} = kf(HA_2 + S_2)[HA_{2free}][S_2] - kb(HA_2 + S_2)[HA_2S_2]$